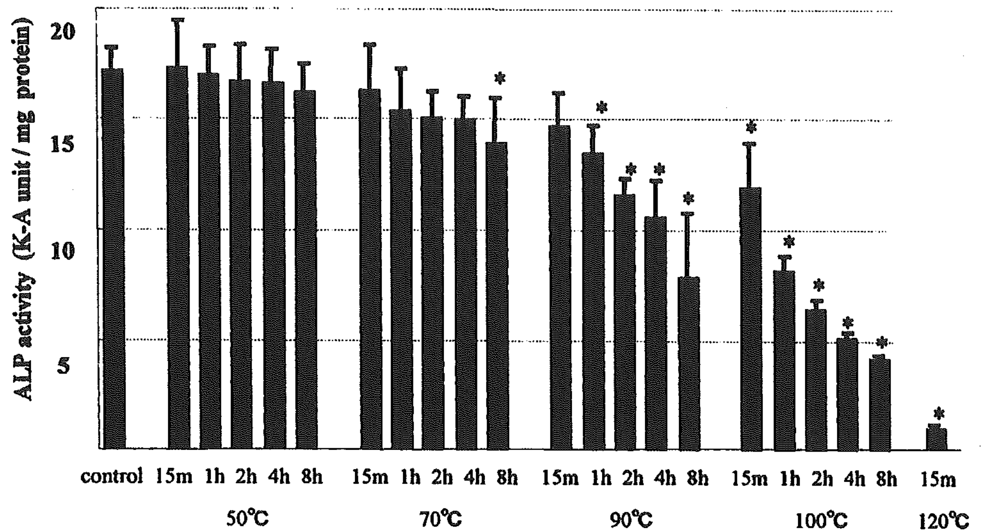

Fig. 1. The influence of heat treatment on rhBMP-2-induced alkaline phosphatase (*ALP*) activity of MC3T3-E1 cells. Data are means ± SD of three culture wells. A significant difference from the control is indicated as * ($P < 0.05$)

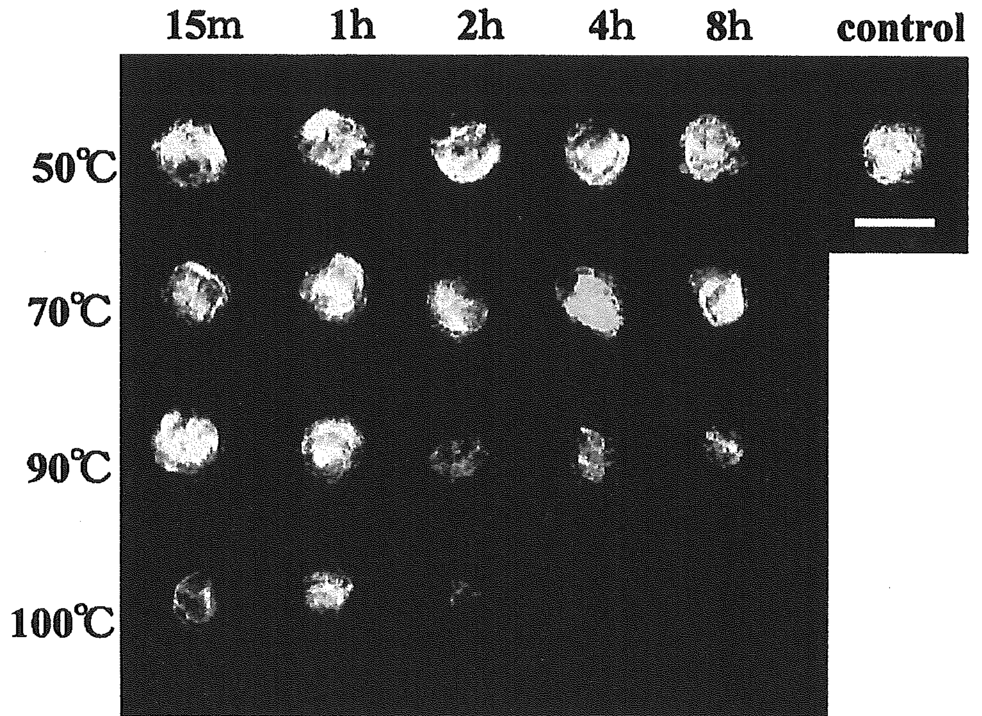

Fig. 2. Soft X-ray photograph of an ossicle formed at 3 weeks after implantation. A typical implant from each group is shown. *Scale bar* = 6 mm. There is no difference in the trabecular pattern within ossicles from each group. However, a reduction in size was observed over 90°C in a time-dependent manner. In the groups heated at 100°C for 4 h, at 100°C for 8 h, and at 120°C for 15 min, there was no firm mass around the implant location. Thus, we decided not to collect tissues from these areas for further analysis (softex and bone mineral content)

Results

Effects on ALP expression by heated rhBMP-2

Figure 1 shows the effects of the heat treatment on the ALP-inducing activity of rhBMP-2 in MC3T3-E1 cells. ALP-inducing activity was preserved at 50°C even after the rhBMP-2 was heated at this temperature for 8 h. A notable reduction in the ALP-inducing activity of rhBMP-2 was seen using protein samples heated at 70°C for 8 h. At 90°C, a significant reduction of activity was noted by heating for 1 h or more in a time-dependent manner. By heating at 100°C, the time-dependent reduction was profound. The ALP-inducing activity was reduced to less than 1 unit/mg protein when the rhBMP-2 was heated at 120°C for 15 min.

Change in the bone-inducing activity of rhBMP-2 by heating

Figure 2 shows representative ossicles elicited in mice within a 3-week period by implanting collagen disks impregnated with 5 μg rhBMP-2 heated at 50, 70, 90, or 100°C for 15 min, or for 1, 2, 4, or 8 h. Ossicle size tended to become

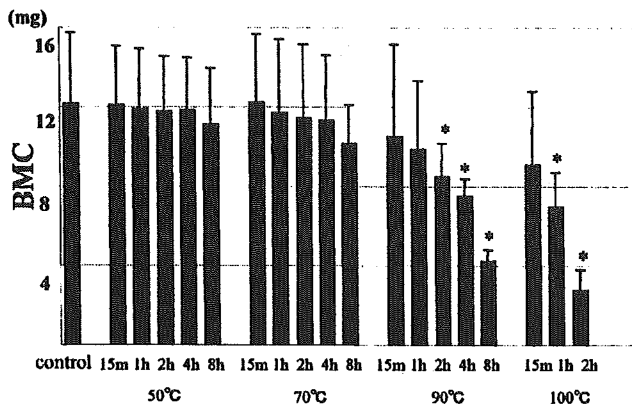

Fig. 3. The bone mineral content (*BMC*) of the tissues harvested at 3 weeks after surgery. Data are means ± SD of 8 samples. A significant difference from the control is indicated as * ($P < 0.05$). There was no significant difference between the BMC of the 50°C and 70°C groups and the control group. However, the mean BMCs of groups heated at 90°C for 2, 4, or 8h and the one heated at 100°C for 1, or 2h ($P < 0.01$) were significantly lower than that found in the control group. In the groups heated at 100°C for 4h, at 100°C for 8h, and at 120°C for 15min, we found no evidence of new ectopic bone formation, as described in the legend to Fig. 2

small when the rhBMP-2 was treated at 90°C for 2h or more. After treatment for more than 4h at 100°C or for 15min at 120°C, the bone-inducing activity of rhBMP-2 was lost.

Figure 3 shows the mean BMC values of the ossicles from each of the groups. The mean (±SD) BMC of the control group was 12.2 ± 3.56mg. In the group treated at 50°C for 8h, the mean BMC was 11.2 ± 2.81mg, which was not significantly lower than that of the controls. In the group with protein heated at 70°C, the mean BMC in the group treated at 70°C for 15min was 12.2 ± 3.45mg. The BMC in the 70°C group showed a downward trend, but no statistically significant difference was observed when compared with the control group. Similarly, in the group using protein heated at 90°C, the BMC of the harvested ossicles decreased with an extension of the heating time. The BMC of ossicles from the groups treated at 90°C for 15min or 90°C for 1h were not significantly different from those of the control group. However, the mean BMC values of the groups treated at 90°C for 2h (8.48 ± 1.68mg), at 90°C for 4h (6.98 ± 1.06mg), or at 90°C for 8h (4.26 ± 0.53mg) were significantly reduced when compared with those of the control group ($P < 0.01$). Again, in the group treated at 100°C for 15min, the BMC was less than that of the controls, although there was no significant difference between the values. The mean BMC of the groups treated at 100°C for 1h (6.96 ± 1.71mg) or at 100°C for 2h (2.80 ± 0.99mg) were significantly lower than those from the control group ($P < 0.01$).

Histological analysis of the ossicles from all groups revealed normal bone histology with hematopoietic marrow and bony trabeculae (Fig. 4).

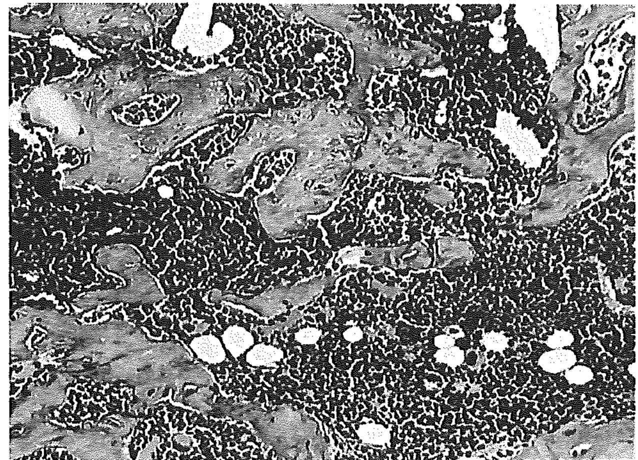

Fig. 4. Photomicrograph of the tissue harvested at 3 weeks after implantation (heated to 50°C for 8h) (H&E, ×200). Normal bone histology with hematopoietic marrow and bony trabeculae was observed

Changes in the SDS-PAGE profile of rhBMP-2 by heating

The SDS-PAGE profiles of rhBMP-2 before and after heating at 90 or 120°C are shown in Fig. 5. The original rhBMP-2 showed three dark bands at around 30-k Daltons (kD) and two light bands below 20kD without DTT (lane 1). With DTT, the 30-kD bands became lighter and the lower molecular-sized bands became darker (lane 4). By heating at 90°C for 2h, in the absence of DTT the 30-kD bands became a little indistinct and two lower sized bands disappeared (lane 2), and with DTT the 30-kD bands became lighter and the lower bands became darker (lane 5). By heating at 120°C for 2h, in the absence of DTT the 30-kD bands remained although the three bands became indistinct (lane 3), and with DTT both of the 30-kD bands and the lower bands were lost (lane 6).

Discussion

BMPs (BMP-2, BMP-7) with potent bone-inducing activity have been successfully produced and developed for clinical use through DNA recombinant technology. Examples of clinical applications include the repair of damaged bone, the reconstruction of bone defects resulting from trauma, and resection of bone tumors. In terms of a successful clinical outcome, the bone-inducing activity of rhBMP-2 must be able to withstand the conditions associated with transportation and storage. In addition, rhBMP has to survive sterilization and the high temperatures encountered when implants are used in close contact with curing bone cement. Previous studies have qualitatively described the stable character of natural BMP based on the ability of crude insoluble BMP-retaining decalcified bone matrix to induce ectopic new bone. Nakanishi et al. [12] reported that rabbit bone-derived BMP extracts elicited ectopic bone after

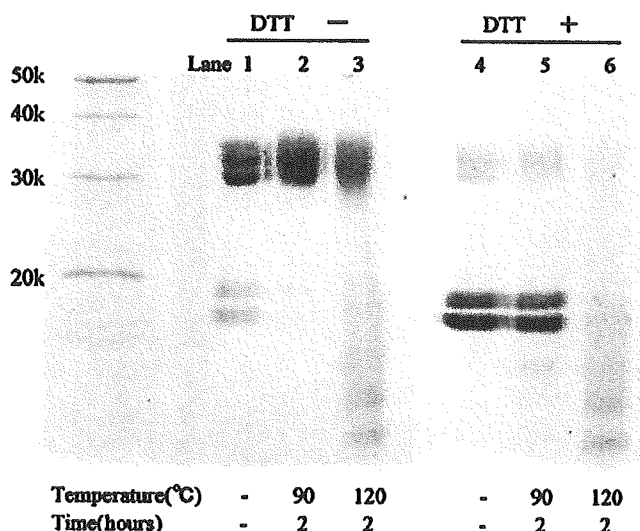

Fig. 5. SDS-PAGE profiles of rhBMP-2 before (*lane 1*) and after (*lane 2*) heating at 90°C and at 120°C (*lane 3*) for 2h. *Lanes 4, 5*, and *6* show the respective samples under reducing conditions in the presence of dithiothreitol (DTT, a disulfide-bond reducing agent). The original rhBMP-2 showed three dark bands at around 30k Daltons (kD) and two light bands below 20kD without DTT (*lane 1*). With DTT, bands at 30kD became lighter and the lower bands became darker (*lane 4*), which indicates that the dimers were reduced to monomers. By heating at 90°C for 2h in the absence of DTT, the major 30-kD bands became a little indistinct, and the two lower-sized bands disappeared (*lane 2*). With DTT, bands at 30kD became lighter and the lower bands became darker (*lane 5*), indicating that the bands at 30kD without DTT maintained a dimeric structure. By heating at 120°C for 2h, the original size of rhBMP-2 was maintained, although the three distinct bands were lost (*lane 3*). With DTT, both of the original 30-kD bands and those lower molecular-sized bands were lost (*lane 6*), indicating complete denaturation of the original configuration of the molecules

heating at 70°C for 10min. However, the bone-inducing activity was lost when the sample was heated at over 100°C for 20min. Some reports have also described similar results using crude BMP extracts as the bone-inducer in rodent models [13,14]. One report demonstrated that BMP activity was retained in a rabbit model after heating the matrix protein at 170°C for 10min or at 140°C for 30min [15].

In this study, the bone mineral content of the rhBMP-2-induced ossicles was used to evaluate the bone-inducing activity of the heat-treated rhBMP-2 in an in vivo system. In addition, the ability of rhBMP-2 to induce ALP activity in osteoblastic cells in culture was used as a model to confirm the results from the in vivo experiments. The ALP-inducing activity of the rhBMP-2 was little affected by heat treatment up to 70°C for 8h or up to 90°C for 1h, but then decreased gradually with increasing temperature and time. The ALP-inducing activity was eventually lost after heating the rhBMP-2 at 120°C, a treatment that denatured the molecular structure of the rhBMP-2 as shown on a SDS-PAGE profile. These results were in accordance with the in vivo results, and suggest that rhBMP-2 is largely stable in nature. The use of autopolymerising polymethylmethacrylate (PMMA)-based bone cement is the most common method chosen for prosthetic component fixation in total joint replacement surgery. During the polymerization of PMMA, high peak temperatures are reached. The temperature peak ranges from 48°C to 105°C at the bone–cement interface, and from 80°C to 124°C in the cement. The exposure time over 50°C is reported to be between 30 and 400s [19]. Thus, the data from the present study suggest that contact with curing bone cement would not affect the bone-inducing activity of rhBMP-2. Sterilizing by autoclave (120°C) would effectively inactivate the biological action of this protein, but sterilizing by ethylene oxide gas (60°C for 3h or 40°C for 6h) would not, as reported previously [20].

The heat-stable character of BMP may be derived from its molecular structure. It is known that the bioactive BMP-2 molecule consists of a homodimer which is essential for its biological activity. The homodimer consists of two 114 amino acid monomers with 7 cysteine residues that form three intramolecular disulfide bonds, with one intermolecular disulfide bond forming a cysteine knot [21]. The heat-resistant nature of the BMP might be explained by the cysteine-knot formation, which is known to contribute to the structural stability of the protein.

The biological activity of the rhBMP was reduced following heat denaturation at 90°C for 2h as evaluated in an in vivo assay system, and for 1h in an in vitro assay system. At these higher temperatures, the reduction in rhBMP-2 activity was temperature- and time-dependent. In order to visualize the heat-dependent changes in molecular structure, changes in the SDS-PAGE gel profile after heating were observed. As previously described, the rhBMP-2 molecule has a molecular size of around 16kD with one N-glycosylation site, and it forms a homodimer which has biological activity [6–8,22]. Therefore, the three bands at 30kD in the control lane on the SDS-PAGE with no disulfide bond reduction indicated dimeric BMP-2 molecules with 2, 1, or no sugar chains, respectively (see Fig. 5). Further, the two faint bands below 20kD were monomers with or without glycosylation because of their similarity to the molecular sizes of the DTT-reduced rhBMP-2 monomer. By heating at 90°C for 2h, in the absence of DTT the dimer bands became a little indistinct and the monomer bands were lost, which indicated complete deformation of the rhBMP-2 monomer. With DTT, the dimer bands became lighter and the monomer bands became darker. These changes most likely reflect partial deformation of the original three-dimensional configuration of the rhBMP-2 dimers, which corresponds with the partial loss of bone inducing activity. A higher temperature (120°C for 2h) made the dimer bands more indistinct and eventually degraded the structure of the monomers, as seen on DTT-reduced SDS-PAGE, with the resultant loss of biological activity.

In conclusion, the biological activity and molecular structure of rhBMP-2 were shown to be fairly resistant to heat treatment. In considering the potential clinical uses of rhBMP-2, the stable character of the protein suggests that it would not need to be cooled during transportation or storage. In addition, it was found that contact with heated material such as curing bone cement would not affect the

bone-inducing activity of the rhBMP-2. However, the autoclaving of rhBMP-2 causes this protein to lose its biological activity based on the results of the present study.

References

1. Celeste AJ, Iannazzi JA, Taylor RC, Hewick RM, Rosen V, Wang EA, Wozney JM (1990) Identification of transforming growth factor beta family members present in bone-inductive protein purified from bovine bone. Proc Natl Acad Sci USA 87:9843–9847
2. Urist MR (1965) Bone formation by autoinduction. Science 150:893–899
3. Urist MR, Iwata H (1973) Preservation and biodegradation of the morphogenetic property of bone matrix. J Theor Biol 38:155–167
4. Reddi AH, Anderson WA (1976) Collagenous bone matrix-induced endochondral ossification hemopoiesis. J Cell Biol 69:557–572
5. Sampath TK, Muthukumaran N, Reddi AH (1987) Isolation of osteogenin, an extracellular matrix-associated, bone-inductive protein, by heparin affinity chromatography. Proc Natl Acad Sci USA 84:7109–7113
6. Wozney JM, Rosen V, Celeste AJ, Mitsock LM, Whitters MJ, Kriz RW, Hewick RM, Wang EA (1988) Novel regulators of bone formation: molecular clones and activities. Science 242:1528–1534
7. Wang EA, Rosen V, Cordes P, Hewick RM, Kriz MJ, Luxenberg DP, Sibley BS, Wozney JM (1988) Purification and characterization of other distinct bone-inducing factors. Proc Natl Acad Sci USA 85:9484–9488
8. Wang EA, Rosen V, D'Alessandro JS, Bauduy M, Cordes P, Harada T, Israel DI, Hewick RM, Kerns KM, LaPan P, Luxenberg DH, McQuid D, Moutsatsos IK, Nove J, Wozney JM (1990) Recombinant human bone morphogenetic protein induces bone formation. Proc Natl Acad Sci USA 87:2220–2224
9. Wozney JM (1992) The bone morphogenetic protein family and osteogenesis. Mol Reprod Dev 32:160–167
10. Takaoka K, Yoshikawa H, Hashimoto J, Miyamoto S, Masuhara K, Nakahara H, Matsui M, Ono K (1993) Purification and characterization of a bone-inducing protein from a murine osteosarcoma (Dunn type). Clin Orthop 292:329–336
11. Takaoka K, Yoshikawa H, Hashimoto J, Masuhara K, Miyamoto S, Suzuki S, Ono K, Matsui M, Oikawa S, Tsuruoka N, Tawaragi Y, Inuzuka C, Katayama T, Sugiyama M, Tsujimoto M, Nakanishi T, Nakazatio H (1993) Gene cloning and expression of a bone morphogenetic protein derived from a murine osteosarcoma. Clin Orthop 294:344–352
12. Nakanishi K, Sato K, Sato T, Takahashi M, Fukaya N, Miura T (1992) Preservation of bone morphogenetic protein in heat-treated bone (in Japanese). Nippon Seikeigeka Gakkai Zasshi (J Jpn Orthop Assoc) 66:949–955
13. Ito T, Sakano S, Sato K, Sugiura H, Iwata H, Murata Y, Seo H (1995) Sensitivity of osteoinductive activity of demineralized and defatted rat femur to temperature and duration of heating. Clin Orthop 316:267–275
14. Inokuchi T, Ninomiya H, Hironaka R, Yoshida S, Araki M, Sano K (1991) Studies on heat treatment for immediate reimplantation of resected bone. J Cranio-Max-Fac Surg 19:31–39
15. Sato T, Iwata H, Takahashi M, Miura T (1993) Heat tolerance of activity toward ectopic bone formation by rabbit bone matrix protein. Ann Chir Gynaecol Suppl 207:37–40
16. Izawa H, Hachiya Y, Kawai T, Muramatsu K, Narita Y, Ban N, Yoshizawa H (2001) The effect of heat-treated human bone morphogenetic protein on clinical implantation. Clin Orthop 390:252–258
17. Dunlop LL, Hall BK (1995) Relationships between cellular condensation, preosteoblast formation and epithelial-mesenchymal interactions in initiation of osteogenesis. Int J Dev Biol 39:357–371
18. Kind PRN, King EJ (1954) Estimation of plasma phosphatase by determination of hydrolyzed phenol with amino-antipyrine. J Clin Pathol 7:322–326
19. Borzacchiello A, Ambrosio L, Nicolais L, Ronca D, Guida G (2001). The temperature at the bone–cement interface: modeling and in vitro analysis. In: Pipino F (ed) Bone Cement and Cemented Fixation of Implants. Zenit, Rome, p 135–140
20. Nawata M, Wakitani S, Nakaya H, Tanigami A, Seki T, Nakamura Y, Saito N, Sano K, Hidaka E, Takaoka K (2005). Use of bone morphogenetic protein-2 and diffusion chambers to engineer cartilage tissue for the repair of defects in articular cartilage. Arthritis Rheum 52:155–163
21. Scheufler C, Sebald W, Hulsmeyer M (1999) Crystal structure of human bone morphogenetic protein-2 at 2.7-A resolution. J Mol Biol 287:103–115
22. Wozney JM (1989) Bone morphogenetic proteins. Prog Growth Factor Res 1:267–280

J Bone Miner Metab (2005) 23:426–434
DOI 10.1007/s00774-005-0624-5

© Springer-Verlag Tokyo 2005

ORIGINAL ARTICLE

**Yukio Nakamura · Shigeyuki Wakitani · Naoto Saito
Kunio Takaoka**

Expression profiles of BMP-related molecules induced by BMP-2 or -4 in muscle-derived primary culture cells

Received: October 7, 2004 / Accepted: April 19, 2005

Abstract The formation of ectopic bone in muscle following the implantation of decalcified bone matrix led to the search and eventual discovery of bone morphogenetic proteins (BMPs) in bone matrix. The precise sequence of molecular events that underpin the cellular transformation of undifferentiated mesenchymal cells into bone has not been established, and is the subject of this study. Northern and Western blot analyses were used to examine changes in gene expression of cells treated with BMP-2 or -4. The molecules, which included BMP receptors (BMPRs), Noggin (a BMP-specific antagonist), osteocalcin (OC), Smad-4, and MyoD, were examined at messenger RNA (mRNA) and protein levels. The changes in expression of these molecules were followed in mouse muscle-derived primary culture cells, and osteoblastic or nonosteoblastic embryonic cell lines. We show the early up-regulation of BMPR-1A, -2, Noggin, OC, and Smad-4 in muscle-derived primary culture cells in a dose-dependent manner in response to BMP-2 or -4. MyoD expression was not detected after BMP stimulation. The differential expression of these positive and negative regulators of BMP signaling points to a potential regulatory mechanism for bone induction in mesenchymal cells.

Key words BMP signaling · Feedback · Mesenchymal cells · Muscle · Up-regulation

Introduction

Bone morphogenetic proteins (BMPs) are multifunctional cytokines belonging to the transforming growth factor-β (TGF-β) superfamily. Among the BMP family, BMP-2, -4, and -7 (osteogenic protein-1) have been recognized as potent bone inducers [1–3], and BMP-2 and -4 also play critical roles in early embryogenesis and skeletal development [4]. Signaling by BMPs requires binding of the BMP (BMP-2, -4, and -7) molecules to the BMP receptors (BMPRs), which consist of two different types of serine-threonine kinase receptors, known as BMP type 1 receptors (1A and 1B) and BMP type 2 receptor [5]. These receptors then phosphorylate intracellular proteins such as the Smad-1 or -5 to effect intracellular signaling and physiological responses [6–9]. Therefore, BMPR expression is a prerequisite for the biological action of the BMPs [1–5]. BMP action may also be modulated by a group of BMP-binding proteins outside the responding cells. Noggin is a representative molecule with such a function, and is assumed to contribute to the negative regulation of BMP action or bone formation under physiological conditions [6–9].

Changes in expression of those molecules involved in BMP signaling are critical to understanding the mechanism of BMP-induced osteogenic differentiation and feedback mechanisms following treatment with BMPs. We previously examined an ectopic bone-forming model in mice [10], and found that BMPR-1A, -2, and Noggin were induced by BMP-2 in muscle tissues during the early phase of the reaction. To confirm this mechanism in in vitro systems, we used muscle-derived primary culture cells, and osteoblastic or non-osteoblastic embryonic cell lines were used as controls.

Y. Nakamura (✉) · S. Wakitani · N. Saito
Department of Orthopaedic Surgery, Shinshu University School of Medicine, 3-1-1 Asahi, Matsumoto 390-8621, Japan
Tel. +81-263-37-2659; Fax +81-263-35-8844

K. Takaoka
Department of Orthopaedic Surgery, Osaka City University Hospital, Osaka, Japan

Materials and methods

Recombinant human BMP-2 (rhBMP-2) and mouse BMP-4 (mBMP-4)

rhBMP-2 was produced by the Genetics Institute (Cambridge, MA, USA) using DNA recombination techniques, and donated to us through Yamanouchi Pharmaceutical (Tokyo, Japan), as described elsewhere [11].

Conditioned media of mBMP-4-transfected Chinese hamster ovary (CHO) cells (BMP-CHO) were the source of mBMP-4. Details of the BMP-CHO cells have been described previously [12,13]. In mBMP-4-conditioned media, the alkaline phosphatase activity of the 10% conditioned media corresponds to approximately 70ng/ml rhBMP-2 [13]. The BMP-CHO cells transfected with mBMP-4 cDNA or mock vector (for a control) were propagated at a density of 1×10^6 cells/100-mm plastic dish (Falcon no. 3003; Becton Dickinson Labware, Tokyo, Japan), and were then cultured in 10ml Dulbecco's modified Eagle's medium (DMEM; Gibco-BRL, Grand Island, NY, USA) with 10% fetal calf serum (FCS; Sigma Chemical, St. Louis, MO, USA) at 37°C for 5 days. The conditioned media were collected after 5 days and stored at 4°C.

Cell culture

Muscle-derived primary culture cells were prepared from the thigh muscles of newborn ddy mice (Nippon SLC, Shizuoka, Japan), as described previously [14], and cultured on a 100-mm plastic dish in DMEM containing 10% (vol/vol:v/v) heat-inactivated FCS and penicillin–streptomycin (PSM) antibiotic mixture (Invitrogen). A murine osteoblastic cell line, MC3T3-E1, and murine embryonic fibroblast-like cell line, NIH3T3, were obtained from the RIKEN Cell Bank (Tsukuba, Japan) and cultured on a 100-mm plastic dish in α-minimal essential medium (Gibco-BRL) and DMEM, respectively, containing 10% (v/v) heat-inactivated FCS.

Experimental protocols

To examine the effects of rhBMP-2 and mBMP-4 on the expression of BMPRs, Noggin, OC, Smad-4, and MyoD in muscle-derived primary culture cells, and MC3T3-E1 and NIH3T3 cells, the culture media were replaced with fresh media containing rhBMP-2 or mBMP-4 at various concentrations (0, 10, 100, 500, 1000, or 1500ng/ml for rhBMP-2, and 0%, 10%, 20%, 40%, 60%, or 80% conditioned media for mBMP-4). The cells were cultured at 37°C in a humidified 5% CO_2 incubator for a period of 6 days, with a change of media on day 3. Cells cultivated for 0, 12, 24, 48, 72, 96, 120, or 144h with each medium containing rhBMP-2 (0, 10, 100, 500, 1000, or 1500ng/ml) or mBMP-4 (0%, 10%, 20%, 40%, 60%, or 80%) were collected and processed for Northern blot analysis. Cells cultivated for 24, 48, 72, or 96h with each medium containing rhBMP-2 (1000 or 1500ng/ml) or mBMP-4 (60% or 80%) were collected and processed for Western blot analysis, as described below.

RNA preparation and reverse transcriptase-polymerase chain reaction (RT-PCR)

Total RNA from primary culture cells derived from embryonic mouse thigh muscle and MC3T3-E1 and NIH3T3 cells was extracted using Isogen (Nippon Gene, Tokyo, Japan) according to the manufacturer's instructions. After treating with RNase-free deoxyribonucleases II (Gibco-BRL), complementary DNA (cDNA) was synthesized using an RNA polymerase chain reaction (PCR) kit (Takara Shuzo, Ohtsu, Japan) according to the manufacturer's instructions. The reaction time was 30min at 42°C. Aliquots of the cDNA pool obtained were subjected to PCR and amplified in a 20μl reaction mixture using *Taq* polymerase (Takara Shuzo). Amplifications were performed in a Program Temp Control System (PC800; ASTEC, Fukuoka, Japan) for 30 cycles after an initial denaturation step at 94°C for 3min, denaturation at 94°C for 30s, annealing for 30s at 60°C, and extension at 72°C for 90s, with a final extension at 72°C for 10min. Reaction products were electrophoresed in a 1.5% agarose gel, and the amplified DNA fragments were visualized by ethidium bromide staining under UV light. PCR products were subcloned and sequenced using a DNA sequencing kit (Applied Biosystems, Warrington, UK). The primers of Noggin, Smad-4, OC, and MyoD for PCR were set as described previously [10,13,15]. The primers of BMPRs for PCR were set as follows: BMPR-1A, 5′-CTCATGTTCAAGGGCAG-3′ (5′ sense) and 5′-CCCCTGCTTGAGATACTC-3′ (3′ antisense; 346–362 and 850–833, respectively); BMPR-1B, 5′-ATGTGGG CACCAAGAAG-3′ and 5′-CTGCTCCAGCCCAATGC T-3′ (215–231 and 681–664, respectively); BMPR-2, 5′-GTGCCCTGGCTGCTATGG-3′ and 5′-TGCCGCCTC CATCATGTT-3′ (47–64 and 592–575, respectively). Nucleotide sequences of the cDNA fragments were checked and found to be identical to mouse BMPRs (BMPR-1A, NM009758; BMPR-1B, NM007560; BMPR-2, NM007561). The specificity of these cDNAs was confirmed by sequencing using an autosequence analyzer (ABI Prism 310 Genetic Analyzer; Perkin-Elmer Japan, Tokyo, Japan).

Northern blot analysis

Twenty micrograms of total RNA were separated by electrophoresis on a 1.0% agarose–formaldehyde gel and blotted onto Hybond-N^+ membrane (Amersham Intl., Piscataway, NJ, USA) for Northern blotting. Filters were hybridized overnight with random-primed [^{32}P]-labeled mouse BMPRs, Noggin, OC, Smad-4, and MyoD cDNA fragment probes at 65°C for 3h in hybridization buffer (50mM Tris-HCl (pH 7.5), 1mg/ml denatured salmon sperm DNA, 1% SDS, 1M NaCl, 10mM EDTA, 0.2% Ficol 400, 0.2% polyvinylpyrolidone, and 0.2% bovine serum albumin) and washed three times with 0.1 × SSC and $NaDodSO_4$ for 1h at 68°C. The signals were detected by a BioImaging Analyzer BAS-1500 (Fuji Photo Film, Tokyo, Japan). For reprobing, each hybridized probe was removed by boiling the membrane in 0.5% SDS, and then sequentially hybridized with the respective target probes.

Western blotting

Muscle-derived primary culture cells, MC3T3-E1 cells, NIH3T3 cells, and mouse skeletal muscle tissue (as a posi-

tive control) were homogenized and dissolved in 0.5 ml sample buffer (0.05 M Tris-HCl (pH 6.8), 2% SDS, 6% β-mercaptoethanol, and 10% glycerol) and centrifuged at 12000 g for 5 min at 4°C. The supernatant was used as the sample, and the protein content of each sample was measured by UV assay at an OD of 280 nm. Anti-mouse Noggin antibody (R&D Systems, Minneapolis, MN, USA) was used at 1 μg/ml. Polyclonal goat antibodies for BMPRs (Santa Cruz, San Diego, CA, USA) were also used at a dilution of 1 μg/ml. Aliquots of protein solution (5 μl) were adjusted to 1 μg/μl, mixed with 1% BPB (1 μl), and then boiled for 2 min and loaded onto each lane of SDS (10%–20%) acrylamide gradient gels (35 mA, low voltage, 90 min). After running the gels, BMPR-1A, -1B, -2, and Noggin proteins in mouse embryo muscle-derived cells, and MC3T3-E1 and NIH3T3 cells, and mouse skeletal muscle tissue were stained with Coomassie brilliant blue (Sigma Chemical). The protein bands were then transferred to polyvinylidene difluoride membrane (Immunobilon-P Transfermembrane, Millipore, Bedford, MA, USA) according to the manufacturer's instructions. After treatment with Blocking Reagent (Nippon Roche, Tokyo, Japan) for 1 h at room temperature, the membranes were washed with PBS for 5 min, and then incubated for 1 h with primary antibody (BMPRs, 1:200; Noggin, 1:100). After two 5-min washes with PBS, the membranes were incubated with peroxidase-conjugated rabbit anti-goat antibody (1:50; Histofine, Nichirei, Tokyo, Japan) for 1 h. After two further 5-min washes with PBS, the immunoblot was developed using an ImmunoStar Kit for Rabbit (Wako Pure Chemical Industries, Tokyo, Japan) to detect biotin and chemiluminescence.

Results

Expression level of messenger RNA (mRNA)

The increase in transcription of BMPR-1A, -2, Noggin, OC, and Smad-4 appeared to be dose-dependent. The expression pattern of these molecules in muscle-derived primary culture cells after 24 h stimulation by rh-BMP-2 or mBMP-4 is shown in Fig. 1. When we performed Northern blotting on all cell sources using 0, 10, 100, 500, 1000, and 1500 ng/ml doses of rhBMP-2, or 0%, 10%, 20%, 40%, 60%, and 80% doses of mBMP-4, the gene expression levels of these molecules were the similar at the following doses: rhBMP-2 (1000 ng/ml), rhBMP-2 (1500 ng/ml), or mBMP-4 (60%) and mBMP-4 (80%). Therefore, the expression of BMPR-1A, -2, Noggin, OC, and Smad-4 appeared to reach a plateau at the 1000 ng/ml dose of rhBMP-2 and 60% mBMP-4. The mRNA expression of these molecules was readily detected at the 10 ng/ml dose of rhBMP-2 and 10% mBMP-4 (Figs. 1 and 2).

The expression levels of BMPR-2 and Noggin mRNA were sharply elevated on day 1, and then decreased gradually in the muscle-derived primary culture cells at all concentrations. Representative expression patterns using rhBMP-2 (100 ng/ml) or mBMP-4 (20%) are shown in Figs. 3A and 4A. BMPR-1A transcription was also elevated on day 1, but at lower levels when compared with BMPR-2 at all concentrations (Figs. 3 and 4).

Similar patterns for BMPR-1A, -2, and Noggin were observed in MC3T3-E1 and NIH3T3 cell lines, but to a much lower degree than that seen in the muscle-derived primary culture cells at all concentrations. The typical expression figures using rhBMP-2 (1000 ng/ml) or mBMP-4 (60%) in MC3T3-E1 and NIH3T3 cell lines are shown in Figs. 5–8. BMPR-1B expression was not detected by Northern blotting before or after BMP stimulation in any cell sources examined, or in OC later on day 4. The Smad-4 mRNA level gradually increased, and reached a plateau from day 2 (Figs. 5–8).

MyoD mRNA expression was detected without BMP-2 or -4 exposure throughout the experimental period. A typical figure in which muscle-derived primary culture cells were stimulated by BMP-2 or -4 after 24 h is shown in Fig. 9A or 9B.

Protein expression levels

Western blotting on the muscle-derived primary culture cells using either 1000 or 1500 ng/ml doses of rhBMP-2, or 60% or 80% of mBMP-4, revealed that the protein expression levels of BMPR-1A, -2, and Noggin were the same at the 1000 ng/ml and 1500 ng/ml doses of rhBMP-2, and at 60% or 80% concentrations of mBMP-4. Therefore, rhBMP-2 (1000 ng/ml) or mBMP-4 (60%) was used for all subsequent studies of protein expression levels in the muscle-derived primary culture cells (Fig. 10). We did not perform Western blotting on MC3T3-E1 and NIH3T3 cell lines because of the weak expression revealed by Northern blotting.

The translational expression levels of BMPR-1A, -2, and Noggin were enhanced on day 2 and then decreased gradually in the muscle-derived primary culture cells. BMPR-1B expression was not detectable by Western blotting before or after BMP stimulation in the muscle-derived primary culture cell (Fig. 10).

Discussion

This study showed increased transcription and translation of BMPR-1A, -2, and Noggin and increased transcription of OC and Smad-4 in response to rhBMP-2 or mBMP-4 in muscle-derived primary culture cells. Clearly, the muscle-derived primary culture cells are capable of responding to changes in the external concentrations of the bone growth factors. Induction of BMPR-1A and -2 following exposure to BMPs points to the activation of a receptor-mediated pathway to effect intracellular signaling by these molecules. Although the reason for the predominant induction of BMPR-2 among BMPRs is unknown at present, it is possible that an increased number of BMPR-2 molecules with a high affinity for BMP might allow greater capture of this

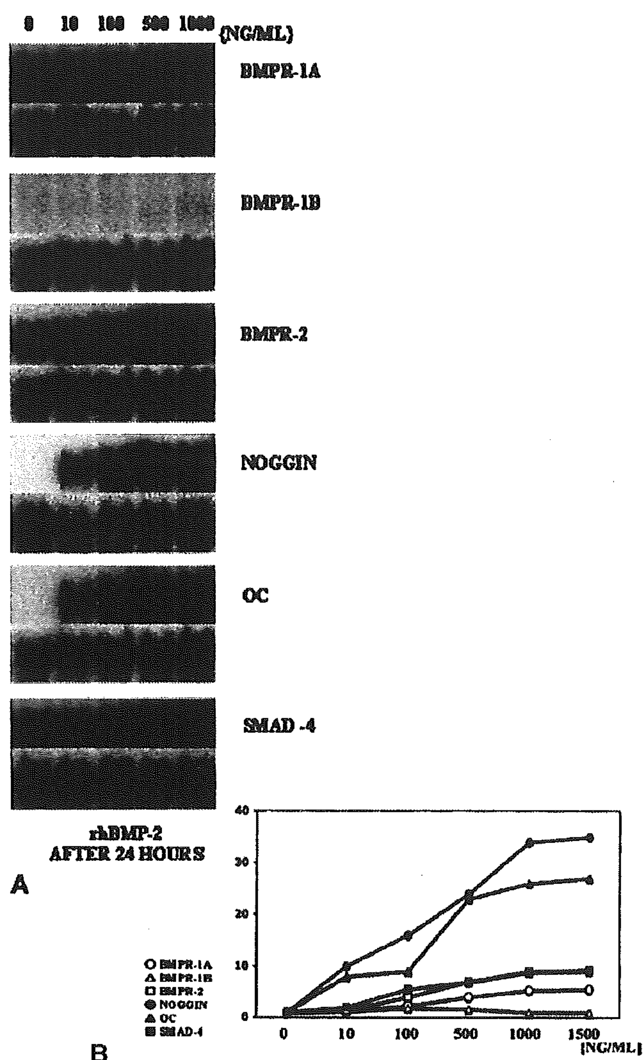

Fig. 1. Gene expression level of BMPR-1A, -1B, -2, Noggin, OC, and Smad-4 after 24-h stimulation of rhBMP-2 (0, 10, 100, 500, 1000 ng/ml) in muscle-derived primary culture cells by Northern blot analysis (**A**) and quantitation of the data of Northern blot analysis by Densitometry (**B**). G3PDH mRNA levels (*the bottoms of all lanes* are G3PDH) obtained by Northern blotting were used for normalization (**A**). The score on hour 0 (just after BMP stimulation) was used as a standard (**B**). BMPR-1A, -2, Noggin, OC, and Smad-4 were up-regulated dose-dependently. No increase in BMPR-1B expression was observed during the course of the study. The expression levels of these molecules were almost the same using 1000 ng/ml and 1500 ng/ml rhBMP-2 (1500 ng/ml rhBMP-2 data not shown in Fig. 1A)

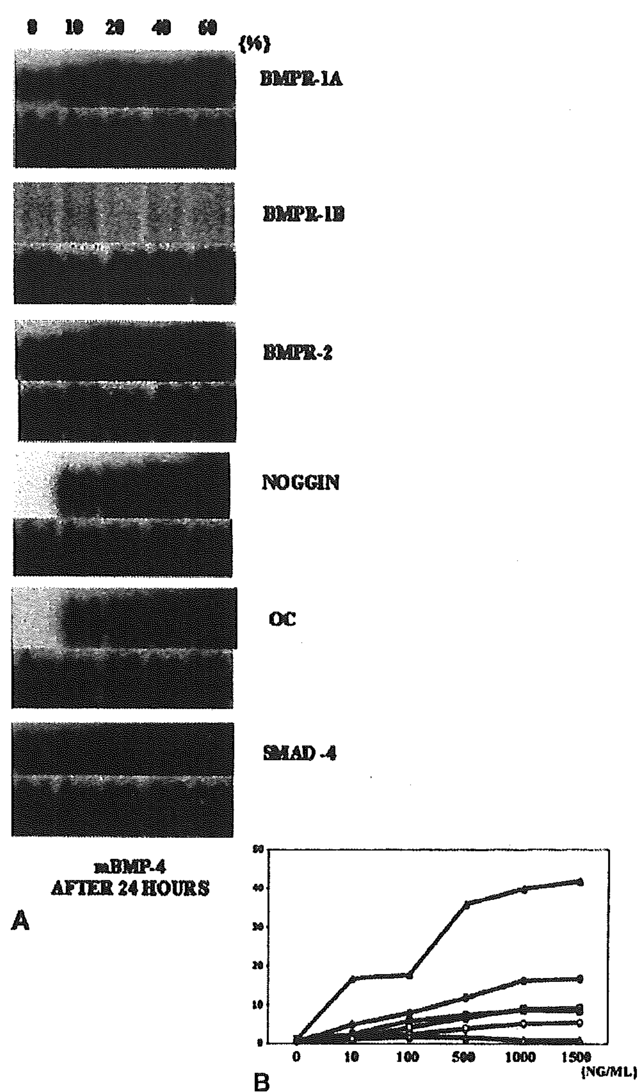

Fig. 2. Gene expression level of BMPR-1A, -1B, -2, Noggin, OC, and Smad-4 after 24-h stimulation of mBMP-4 [0%, 10%, 20%, 40%, and 60% (v/v) conditioned media] in muscle-derived primary culture cells by Northern blot analysis (**A**) and quantitation of the data of Northern blot analysis by Densitometry (**B**). G3PDH mRNA levels (*the bottoms of all lanes* are G3PDH) obtained by Northern blotting were used for normalization (**A**). The score on hour 0 (just after BMP stimulation) was used as a standard (**B**). The gene expression pattern of the molecules after stimulation of mBMP-4 was similar to that observed after stimulation of rhBMP-2. The expression levels of these molecules were almost the same using 60% and 80% mBMP-4. (80% mBMP-4 data not shown in Fig. 2A)

ligand and subsequent activation of BMPR-1A for enhanced transduction of the BMP signal into cells.

We have observed that expression of BMPR-1A and -2 is significantly increased during the early phase of ectopic bone formation following the implantation of rhBMP-2 into the back muscles of adult mice [10]. Based on these data from in vivo and in vitro studies, the activation of BMPR-1A after BMPR-2 might be a key event following BMP stimulation of muscle tissue. BMPR-1A, -2, and Noggin were induced in MC3T3-E1 and NIH3T3 cell lines, but to a much lesser degree than that seen in the muscle-derived primary culture cells used in this study.

A specific role of BMPR-1B in skeletal development has been proposed based on the abnormal interphalangeal joint formation in an animal with a null mutation in this receptor. However, the expression of BMPR-1B appeared to be limited in the muscle-derived primary culture cells and the osteoblastic or nonosteoblastic embryonic cell lines, even after exposure to BMPs [16–19]. The lack of expression of BMPR-1B was in accordance with results in a previous

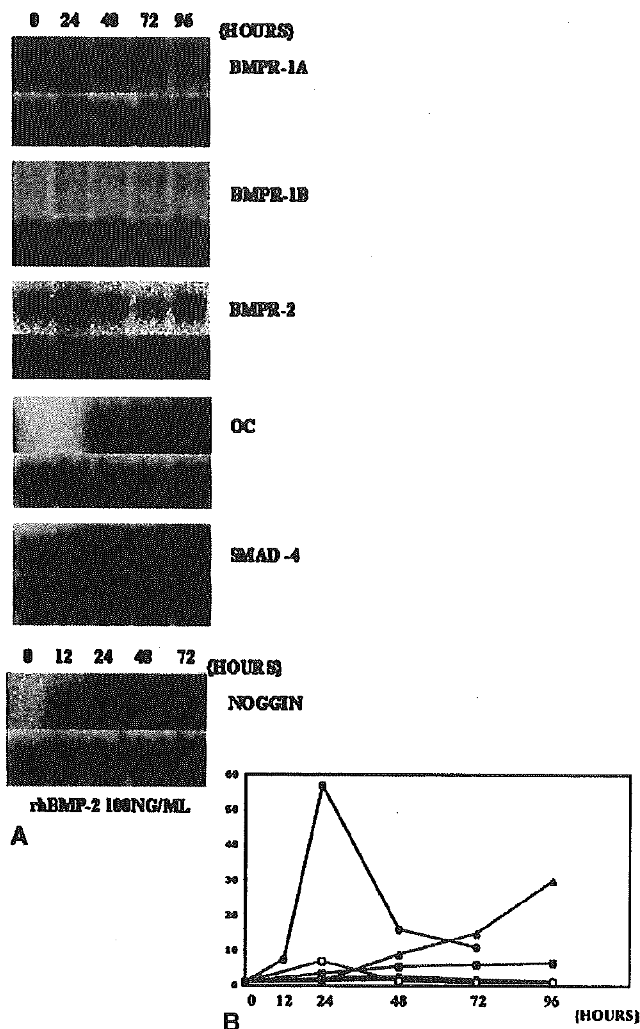

Fig. 3. Gene expression of BMPR-1A, -1B, -2, OC, and Smad-4 for 0, 24, 48, 72, and 96 h and Noggin for 0, 12, 24, 48, and 72 h after 100 ng/ml rhBMP-2 stimulation in muscle-derived primary culture cells by Northern blot analysis (**A**) and quantitation of the data of Northern blot analysis by Densitometry (**B**). G3PDH mRNA levels (*the bottoms of all lanes* are G3PDH) obtained by Northern blotting were used for normalization (**A**). The score on hour 0 (just after BMP stimulation) was used as a standard (**B**). After rhBMP-2 stimulation, OC was up-regulated time-dependently. Noggin level peaked at 24 h. Expression of BMPR-1A and -2 was increased moderately after 24 h, then gradually decreased thereafter. Smad-4 was gradually and weakly up-regulated after stimulation. BMPR-1B was not increased during the experimental period

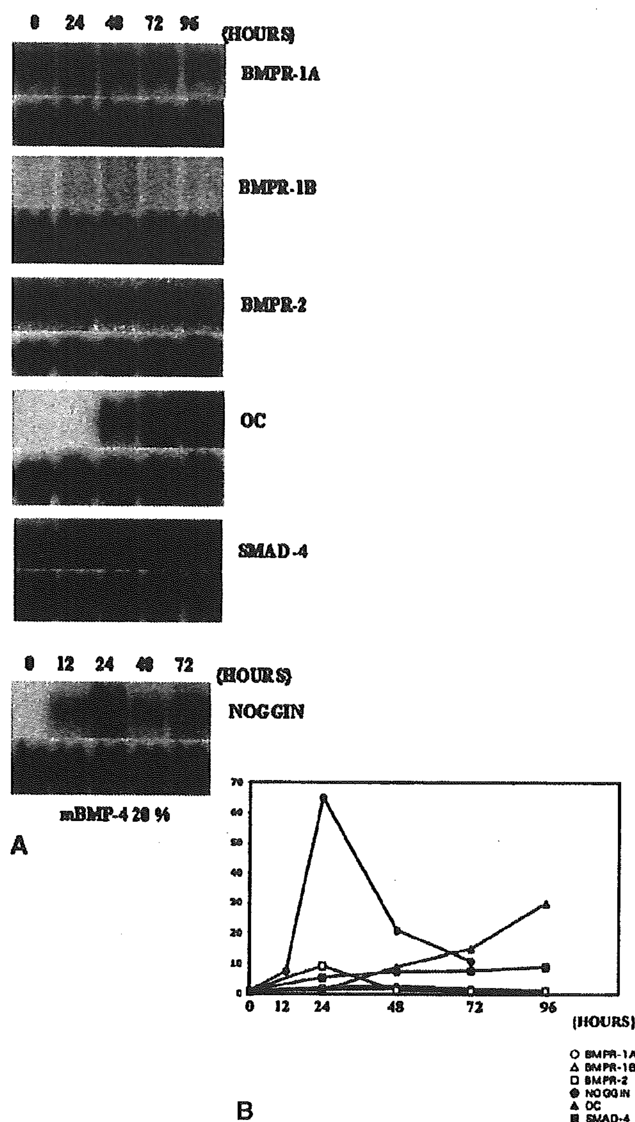

Fig. 4. Gene expression of BMPR-1A, -1B, -2, OC, and Smad-4 for 0, 24, 48, 72, and 96 h and Noggin for 0, 12, 24, 48, and 72 h after 20% mBMP-4 stimulation in muscle-derived primary culture cells by Northern blot analysis (**A**) and quantitation of the data of Northern blot analysis by Densitometry (**B**). G3PDH mRNA levels (*the bottoms of all lanes* are G3PDH) obtained by Northern blotting were used for normalization (**A**). The score on hour 0 (just after BMP stimulation) was used as a standard (**B**). The gene expression pattern of the molecules after stimulation of mBMP-4 (20%) was similar to that seen after stimulation of 100 ng/ml rhBMP-2

report using the pluripotent C2C12 cell line, and another study that revealed predominant expression of BMPR-1B in brain and not skeleton [20].

The induction of Noggin gene expression in cells of the osteoblastic lineage following exposure to rhBMP-2, and in fetal rat limb explants by BMP-7, has been reported [21,22]. In this study, Noggin gene expression was also confirmed in muscle-derived primary culture cells, an osteoblastic cell line (MC3T3-E1), and a nonosteoblastic, embryonic fibroblast-like cell line (NIH3T3) [16,23,24]. As Noggin is a representative antagonist of BMP action, the expression of Noggin might act as a negative regulator of the BMP-induced cellular reactions, and consequently reduce the susceptibility of the cells to BMPs.

Three classes of Smads, termed receptor-activated Smads (R-Smads), common Smads (Co-Smads), and inhibitory Smads (I-Smads), have been identified in mammals. Smads1, 5, and 8 are R-Smads that primarily mediate BMP signaling from the receptors to the nucleus [16,25]. Therefore, the up-regulation of Smad-4, which is a representative BMP signaling Co-Smad, in a time- or dose-

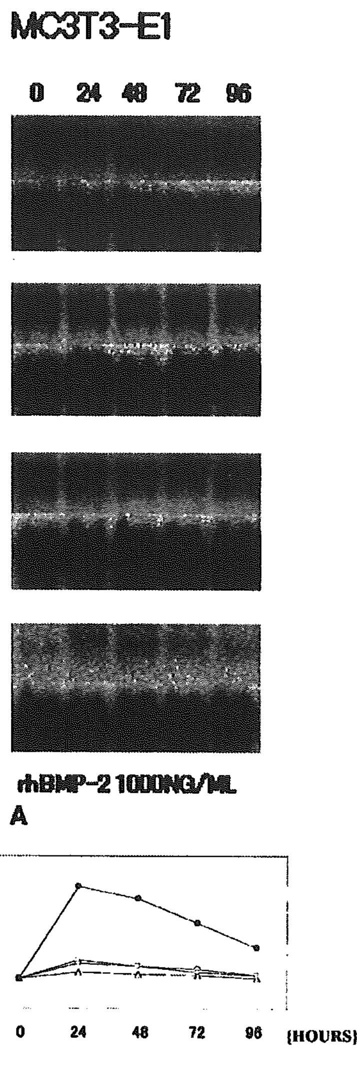

Fig. 5. Gene expression of BMPR-1A, -1B, -2, and Noggin for 0, 24, 48, 72, and 96h after 1000ng/ml rhBMP-2 stimulation in MC3T3-E1 cell line by Northern blot analysis (A) and quantitation of the data of Northern blot analysis by Densitometry (B). G3PDH mRNA levels (*the bottoms of all lanes* are G3PDH) obtained by Northern blotting were used for normalization (A). The score on hour 0 (just after BMP stimulation) was used as a standard (B). BMPR-1A and -2 were weakly induced after rhBMP-2 stimulation, peaked at 24h, then decreased gradually. Noggin was also moderately induced after stimulation showed maximal expression at 24h, then decreased thereafter. BMPR-1B was not induced during the course of the reaction

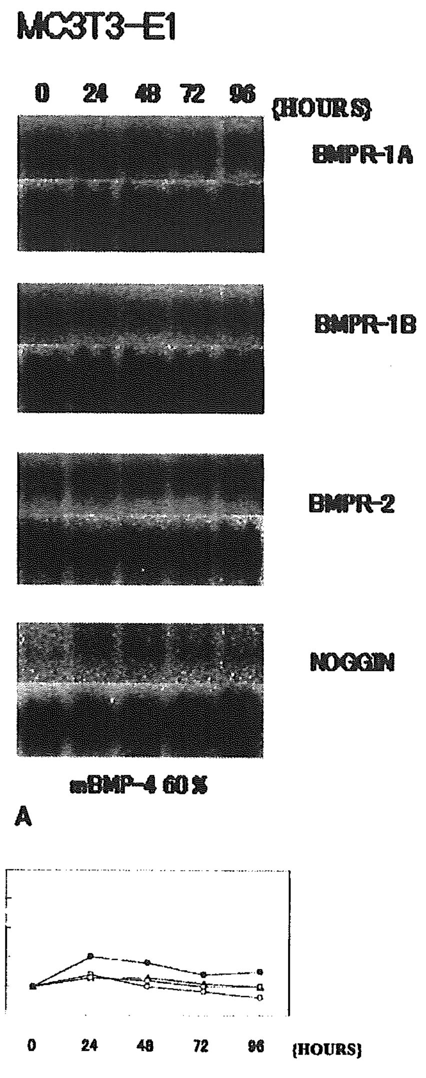

Fig. 6. Gene expression of BMPR-1A, -1B, -2, and Noggin for 0, 24, 48, 72, and 96h after mBMP-4 (20%) stimulation in MC3T3-E1 cell line by Northern blot analysis (A) and quantitation of the data of Northern blot analysis by Densitometry (B). G3PDH mRNA levels (*the bottoms of all lanes* are G3PDH) obtained by Northern blotting were used for normalization (A). The score on hour 0 (just after BMP stimulation) was used as a standard (B). The gene expression pattern of the molecules after stimulation of mBMP-4 (20%) was similar to that seen after stimulation of 1000ng/ml rhBMP-2, but the expression levels with mBMP-4 (20%) were smaller than those with 1000ng/ml rhBMP-2

dependent manner suggests that BMP signaling in muscle tissue is regulated in a coordinated manner. OC is a well-characterized osteoblast differentiation marker, and MyoD is also a good marker for myoblastic differentiation [26]. Although the expression of MyoD was not detected in this study, the expression of OC was enhanced on day 2 after BMP-2 or -4 stimulation. These results indicate that BMP-induced osteogenic differentiation in muscle tissue might occur through a BMP/Smad signaling pathway, and muscle-derived primary culture cells might lose the muscle phenotype after BMP exposure.

The expression profiles were much more prominent for primary undifferentiated mesenchymal cells derived from muscle than for MC3T3-E1 or NIH3T3 cells in this study. Muscle-derived primary culture cells include a large population of undifferentiated mesenchymal cells, as described elsewhere [14]. Clearly, undifferentiated mesenchymal cells in muscle tissue are highly responsive to BMPs, based on

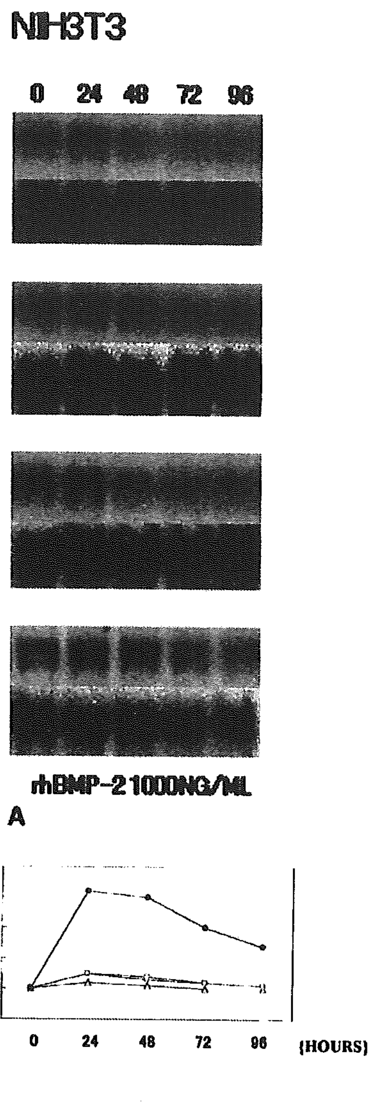

Fig. 7. Gene expression of BMPR-1A, -1B, -2, and Noggin for 0, 24, 48, 72, and 96h after 1000ng/ml rhBMP-2 stimulation in NIH3T3 cell line by Northern blot analysis (**A**) and quantitation of the data of Northern blot analysis by Densitometry (**B**). G3PDH mRNA levels (*the bottoms of all lanes* are G3PDH) obtained by Northern blotting were used for normalization (**A**). The score on hour 0 (just after BMP stimulation) was used as a standard (**B**). BMPR-1A and -2 were weakly induced after rhBMP-2 stimulation, peaked at 24h, then decreased gradually. Noggin was moderately induced after stimulation showed maximal expression at 24h, then decreased thereafter

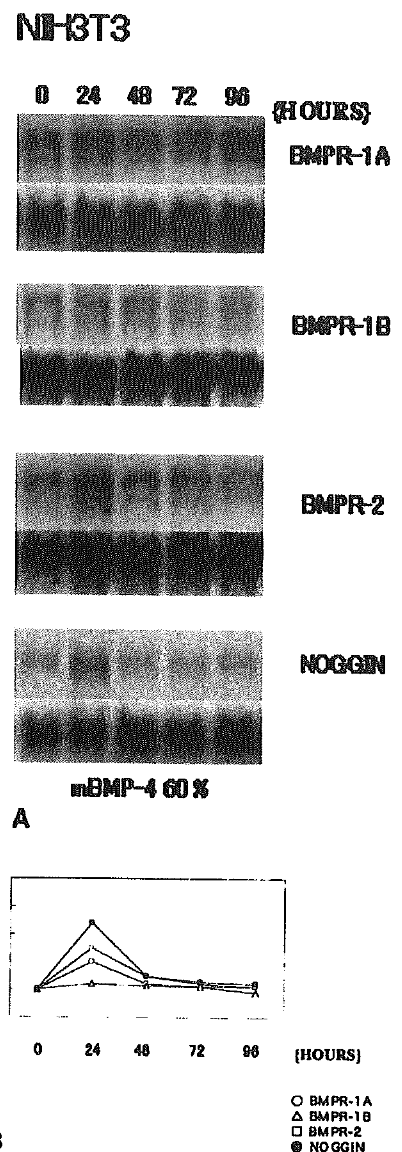

Fig. 8. Gene expression of BMPR-1A, -1B, -2, and Noggin for 0, 24, 48, 72, and 96h after mBMP-4 (20%) stimulation in NIH3T3 cell line by Northern blot analysis (**A**) and quantitation of the data of Northern blot analysis by Densitometry (**B**). G3PDH mRNA levels (*the bottoms of all lanes* are G3PDH) obtained by Northern blotting were used for normalization (**A**). The score on hour 0 (just after BMP stimulation) was used as a standard (**B**). BMPR-1A and -2 were weakly induced after rhBMP-2 stimulation, peaked at 24h, then decreased gradually. Noggin was moderately induced after stimulation showed maximal expression at 24h, then decreased thereafter. BMPR-1B was not induced in all experimental stages. In NIH3T3 cells, the expression pattern was similar to that observed in the MC3T3-E1 culture experiments. Expression levels were greater in NIH3T3 cells than in MC3T3-E1 cells

the changes in gene and protein expression levels observed in this study. The proliferation and differentiation of osteoblasts from osteoprogenitor cells in murine bone marrow cultures induced by BMP-2 or -4 have been reported [27,28]. However, there have been few reports using muscle-derived primary culture cells with BMPs. In this study, the expression of BMP-related molecules was examined using undifferentiated mesenchymal cells derived from mouse muscle tissue.

The majority of undifferentiated mesenchymal cells in muscle-derived primary culture cells showed a fibroblastic appearance. These cells are considered to be heterogenous, and contain some kinds of precursor cells such as bone, cartilage, and muscle. They differentiate into each phenotype when they are placed in each differentiation condition.

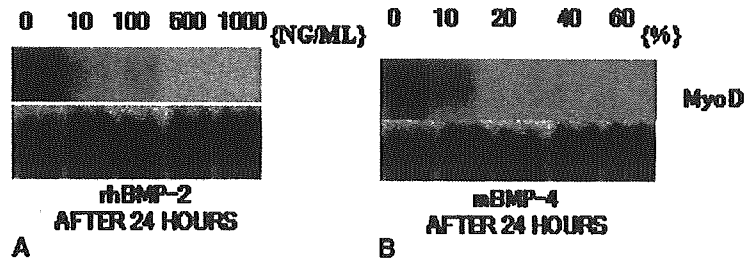

Fig. 9. The expression of MyoD in muscle-derived primary culture cells by Northern blot analyses. G3PDH mRNA levels obtained by Northern blotting were used for normalization. The expression of MyoD mRNA was not detected after BMP-2 or -4 exposure, and the expression was detected only at 0 and 24 h, and not after 24 h BMP stimulation

Fig. 10. Western blot analysis of BMPR-1A, -1B, -2, and Noggin after 60% mBMP-4 or 1000 ng/ml rhBMP-2 stimulation in muscle-derived primary culture cells. Equivalent loading and integrity of protein were confirmed by Coomassie brilliant blue staining on the gel (*lower panel*). Mouse skeletal muscle proteins were used as positive controls. BMPR-1A and -2 were detected at 0 h, induced at 24 h, peaked at 48 h, and then gradually decreased in both 60% mBMP-4 and 1000 ng/ml rhBMP-2 stimulation groups. Expression was greater for BMPR-2 than for BMPR-1A. BMPR-1B was not detectable during any stages in either treatment group. Noggin was not detected at 0 h, was up-regulated at 24 h, peaked at 48 h, and decreased thereafter

In our study, BMPs stimulated them to upregulate the expressions of a bone marker (OC) and cartilage markers (type II collagen and aggrecan, data not shown), but not the muscle marker examined previously. However, it is unclear whether bone and cartilage phenotypes were induced by BMPs in separate cells or in a single cell.

To further understand the potential autoregulatory mechanism in response to BMP, further gene expression

studies will be necessary. Ultimately, this knowledge may provide new approaches to the regulation of local and systemic bone formation.

References

1. Aspenberg P, Turek T (1996) BMP-2 for intramuscular bone induction: effect in squirrel monkeys is dependent on implantation site. Acta Orthop Scand 67:3–6
2. Itoh H, Ebara S, Kamimura M, Tateiwa Y, Kinoshita T, Yuzawa Y, Takaoka K (1999) Experimental spinal fusion with use of recombinant human bone morphogenetic protein. 2. Spine 24:1402–405
3. Takaoka K, Yoshikawa H, Hashimoto J, Ono K, Matsui M, Nakazato H (1994) Transfilter bone induction by Chinese hamster ovary (CHO) cells transfected by DNA encoding bone morphogenetic protein-4. Clin Orthop 300:269–273
4. Kaplan FS, Shore EM (1999) Illustrative disorders of ectopic skeletal morphogenesis: a childhood parallax for studies in gravitational and space biology. Gravit Space Biol Bull 12:27–38
5. Miyazono K, Ichijo H, Heldin CH (1993) Transforming growth factor-beta: latent forms, binding proteins and receptors. Growth Factors 8:11–22
6. Fujii M, Takeda K, Imamura T, Aoki H, Sampath TK, et al. (1999) Roles of bone morphogenetic protein type I receptors and Smad proteins in osteoblast and chondroblast differentiation. Mol Biol Cell 10:3801–3813
7. Ishidou Y, Kitajima I, Obama H, Maruyama I, Murata F, et al. (1995) Enhanced expression of type I receptors for bone morphogenetic proteins during bone formation. J Bone Miner Res 10: 1651–1659
8. Onishi T, Ishidou Y, Nagamine T, Yone K, Iamamura T, et al. (1998) Distinct and overlapping patterns of localization of bone morphogenetic protein (BMP) family members and a BMP type II receptor during fracture healing in rats. Bone 22:605–612
9. Kaneko H, Arakawa T, Mano H, Kaneda T, Ogasawara A, et al. (2000) Direct stimulation of osteoclastic bone resorption by bone morphogenetic protein (BMP)-2 and expression of BMP receptors in mature osteoclasts. Bone 27:479–486
10. Nakamura Y, Wakitani S, Nakayama J, Wakabayashi S, Horiuchi H, Takaoka K (2003) Temporal and spatial expression profiles of BMP receptors and Noggin during BMP-2-induced ectopic bone formation. J Bone Miner Res 18:1854–1862
11. Horiuchi H, Saito N, Kinoshita T, Wakabayashi S, Tsutsumimoto T, Takaoka K (2001) Enhancement of bone morphogenetic protein-2-induced new bone formation in mice by the phosphodiesterase inhibitor pentoxifylline. Bone 28:290–294
12. Takaoka K, Yoshikawa H, Hashimoto J, Ono K, Matsui M, Nakazato H (1994) Transfilter bone induction by Chinese hamster ovary (CHO) cells transfected by DNA encoding bone morphogenetic protein-4. Clin Orthop 300:269–273
13. Tsutsumimoto T, Wakabayashi S, Kinoshita T, Horiuchi H, Takaoka K (2002) A phosphodiesterase inhibitor, pentoxifylline, enhances the bone morphogenetic protein-4 (BMP-4)-dependent differentiation of osteoprogenitor cells. Bone 31:396–401
14. Yaffe D (1973) Rat skeletal muscle cells. In: Kruse PF, Patterson MK (eds) Tissue Culture, vol 16. Academic Press, New York, p 106–114
15. Yoshimura Y, Nomura S, Kawasaki S, Tsutsumimoto T, Shimizu T, Takaoka K (2001) Colocalization of Noggin and bone morphogenetic protein-4 during fracture healing. J Bone Miner Res 16:876–884
16. Kamiya N, Jikko A, Kimata K, Damsky C, Shimizu K, Watanabe H (2002) Establishment of a novel chondrocytic cell line N1511 derived from p53-null mice. J Bone Miner Res 17:1832–1842
17. Jiao K, Zhou Y, Hogan BL (2002) Identification of mZnf8, a mouse Kruppel-like transcriptional repressor, as a novel nuclear interaction partner of Smad1. Mol Cell Biol 22:7633–7644
18. Yamaguchi A, Ishizuya T, Kitou N, Wada Y, Katagiri T, et al. (1996) Effects of BMP-2, BMP-4, and BMP-6 on osteoblastic differentiation of bone marrow-derived stromal cell lines, ST2 and MC3T3-G2/PA6. Biochem Biophys Res Commun 220:366–371
19. Zhao M, Harris SE, Horn D, Geng Z, Nishimura R, Mundy GR, Chen D (2002) Bone morphogenetic protein receptor signaling is necessary for normal murine postnatal bone formation. J Cell Biol 157:1049–1060
20. Wlodarski KH, Reddi AH (1986) Importance of skeletal muscle environment for ectopic bone induction in mice. Folia Biol (Krakow) 34:425–434
21. Chen D, Ji X, Harris MA, Feng JQ, Karsenty G, et al. (1998) Differential roles for bone morphogenetic protein (BMP) receptor type 1B and 1A in differentiation and specification of mesenchymal precursor cells to osteoblast and adipocyte lineages. J Cell Biol 142:295–305
22. Akiyama S, Katagiri T, Namiki M, Yamaji N, Yamamoto N, et al. (1997) Constitutively active BMP type I receptors transduce BMP-2 signals without the ligand in C2C12 myoblasts. Exp Cell Res 235:362–369
23. Gazzerro E, Gangji V, Canalis E (1998) Bone morphogenetic proteins induce the expression of Noggin, which limits their activity in cultured rat osteoblasts. J Clin Invest 15:2106–2114
24. Nifuji A, Noda M (1999) Coordinated expression of Noggin and bone morphogenetic proteins (BMPs) during early skeletogenesis and induction of Noggin expression by BMP-7. J Bone Miner Res 14:2057–2066
25. Attisano L, Tuen Lee-Hoeflich S (2001) The Smads Genome. Biol 2:Reviews3010
26. Yamamoto N, Akiyama S, Katagiri T, Namiki M, Kurosawa T, Suda T (1997) Smad1 and smad5 act downstream of intracellular signalings of BMP-2 that inhibits myogenic differentiation and induces osteoblast differentiation in C2C12 myoblasts. Biochem Biophys Res Commun 238:574–580
27. Zou H, Wieser R, Massague J, Niswander L (1997) Distinct roles of type I bone morphogenetic protein receptors in the formation and differentiation of cartilage. Genes Dev 11:2191–2203
28. Abe E, Yamamoto M, Taguchi Y, Lecka-Czernik B, O'Brien CA, et al. (2000) Essential requirement of BMPs-2/4 for both osteoblast and osteoclast formation in murine bone marrow cultures from adult mice: antagonism by Noggin. J Bone Miner Res 15:663–673

ARTHRITIS & RHEUMATISM
Vol. 52, No. 2, February 2005, pp 637–641
DOI 10.1002/art.20794
© 2005, American College of Rheumatology

Use of Local Electroporation Enhances Methotrexate Effects With Minimum Dose in Adjuvant-Induced Arthritis

Masahiro Tada, Kentaro Inui, Tatsuya Koike, and Kunio Takaoka

Objective. **To investigate the effects of electrical pulses on the ability of methotrexate (MTX) to attenuate inflammation and subsequent joint destruction in rats with adjuvant-induced arthritis (AIA).**

Methods. **Rats in the experimental group received an intraperitoneal injection of MTX (0.125 mg/kg body weight), followed 30 minutes later by application of direct electrical pulses (50V, 8 Hz) to their left hind paws with an electroporation apparatus (M+/E+ group; n = 8). The procedure was repeated twice weekly for 3 weeks. Three control groups received the following treatments, respectively: MTX without electrical treatment (M+/E− group; n = 9), electrical treatment but no MTX (M−/E+ group; n = 10), or no electrical treatment and no MTX (M−/E− group; n = 9). Progression of AIA was monitored by joint swelling and radiologic and histologic changes in the ankle joint.**

Results. **Three weeks after injection of the adjuvant, and at the height of the arthritic reaction, the swelling and radiologic and histologic changes in the left hind paws in the M+/E+ rats were significantly reduced, as compared with changes observed in the control groups.**

Conclusion. **These results demonstrate that application of electrical pulses in combination with use of systemic low-dose MTX can ameliorate local arthritic reactions. This response probably occurs because electrical stimulation promotes transient passage of MTX through pores in the cell membranes, with a resultant local increase in the concentration of the drug within the cells. These results point to a potential use of electrochemotherapy to increase the efficacy of MTX or other drugs in an arthritic joint that is refractory to treatment, without increasing the dose of the drug.**

Although new biologic agents (1) can ameliorate inflammatory reactions and consequently protect the joints of patients with rheumatoid disease from progressive damage (2), methotrexate (MTX) remains one of the most effective and widely used disease-modifying antirheumatic drugs (DMARDs) (3). However, chronic inflammation often persists in isolated joints even after effective systemic MTX treatment, presumably as a result of an inadequate concentration of MTX in the joint that is refractory to treatment. In patients with persistent inflammation, synovectomy is often indicated for symptomatic relief, although data on the long-term clinical effectiveness of this approach are limited (4). Another option is an additional dose of MTX, but this increases the risk of adverse events. Because MTX has weak cell permeability, and the pharmacologic effects of this drug depend upon its intracellular concentration, any method for increasing intracellular MTX levels in the joint may be effective in attenuating the inflammatory response.

Electroporation has been used to facilitate the transport of nonpermeable molecules into cells. Transient cell membrane pores, generated electrically, allow nonpermeable molecules, including genes and drugs, to enter into the cells (5). Electroporation systems are now available for clinical use to deliver anticancer drugs into malignant solid tumor cells (6–8) as electrochemotherapy. Encouraging clinical results have been reported for the treatment of malignancies, in terms of efficacy, safety, and cost (9). This suggests that electroporation may be useful for the local treatment of rheumatoid arthritis (RA) that is refractory to conventional therapy.

We used electroporation to enhance the effect of

Supported by the Ministry of Education, Culture, Sports, Science and Technology of Japan (grant-in-aid 15591594).

Masahiro Tada, MD, Kentaro Inui, MD, PhD, Tatsuya Koike, MD, PhD, Kunio Takaoka, MD, PhD: Osaka City University, Graduate School of Medicine, Osaka, Japan.

Address correspondence and reprint requests to Masahiro Tada, MD, Department of Orthopaedic Surgery, Osaka City University, Graduate School of Medicine, 1-4-3 Asahimachi, Abeno-ku, Osaka 545-8585, Japan. E-mail: m-tada@med.osaka-cu.ac.jp.

Submitted for publication May 11, 2004; accepted in revised form October 21, 2004.

low-dose MTX treatment on the progression to severe arthritis and associated joint destruction in a rat model of adjuvant-induced arthritis (AIA) (10–12).

MATERIALS AND METHODS

Animals. Inbred 7-week-old male Lewis rats were purchased from Charles River Japan (Kanagawa, Japan) and housed with free access to standard laboratory chow and water, under 12-hour dark/light cycles in conditioned air.

Induction of arthritis. The adjuvant mixture was prepared by mixing dried heat-killed *Mycobacterium butyricum* (Difco, Detroit, MI) in paraffin oil (Wako, Tokyo, Japan) at a concentration of 5 mg/ml. To induce systemic arthritis, 0.2 ml of the preparation was injected into the tail bases of 8-week-old rats that had received anesthesia via ethyl ether inhalation.

Pulsed electrical stimulation for electroporation. For electrical stimulation to generate transient pores in cell membranes at the target tissue site, we used an electroporation apparatus (CUY-21; Gene System, Osaka, Japan). Direct-current electrical pulses (8 Hz, 75 msec pulse duration, 50 volts/cm electrode distance) of 1-second duration were delivered 6 times during a single procedure. Each of the six 1-second pulses was applied by 2 parallel stainless steel electrodes that were moved between each pulse through 60° in a plane perpendicular to the long axis of the left hind paws, 30 minutes after an intraperitoneal injection of MTX or saline. We used electrode paste (Gelaid; Nihon Koden, Tokyo, Japan) to prevent skin burns.

Experimental protocol. The animals were assigned to an experimental group or to 1 of 3 control groups, as follows: MTX injection with electroporation (M+/E+ [experimental] group; n = 8), MTX without electroporation (M+/E− group; n = 9), electroporation with saline (M−/E+ group; n = 10), or no treatment (M−/E− group; n = 9).

MTX was provided by Wyeth-Pharmaceutical (Tokyo, Japan). The dose of MTX was set to 0.125 mg/kg body weight, based on preliminary experimental data indicating that no significant systemic antiarthritic changes were recognized at this dose. The drug was administered intraperitoneally twice weekly for 3 weeks, and the animals were killed by asphyxia in carbon dioxide (for radiologic and histologic examination).

These experimental protocols were in accordance with institutional regulations for animal care and were approved by the Institutional Committee for Animal Care of Osaka City University.

Gross inspection and radiologic evaluation. Twice weekly, the animals were weighed using an electronic balance, and hind paw thickness was measured with digital calipers. Three weeks after the adjuvant was injected, the animals were killed using CO_2 asphyxiation, and both hind limbs were harvested and fixed by perfusing cold 4% paraformaldehyde through the left ventricle, followed by immersion in cold 4% paraformaldehyde solution. Soft x-ray images of the hind paws were obtained with a soft x-ray apparatus (DCS-600EX; Aloka, Tokyo, Japan) using settings of 45 kV, 4 mA, and 30 seconds of exposure time. Destructive changes in hind paw bones seen on radiographs were evaluated by criteria previously described by Clark et al (13), with some modifications. Briefly, radiographic

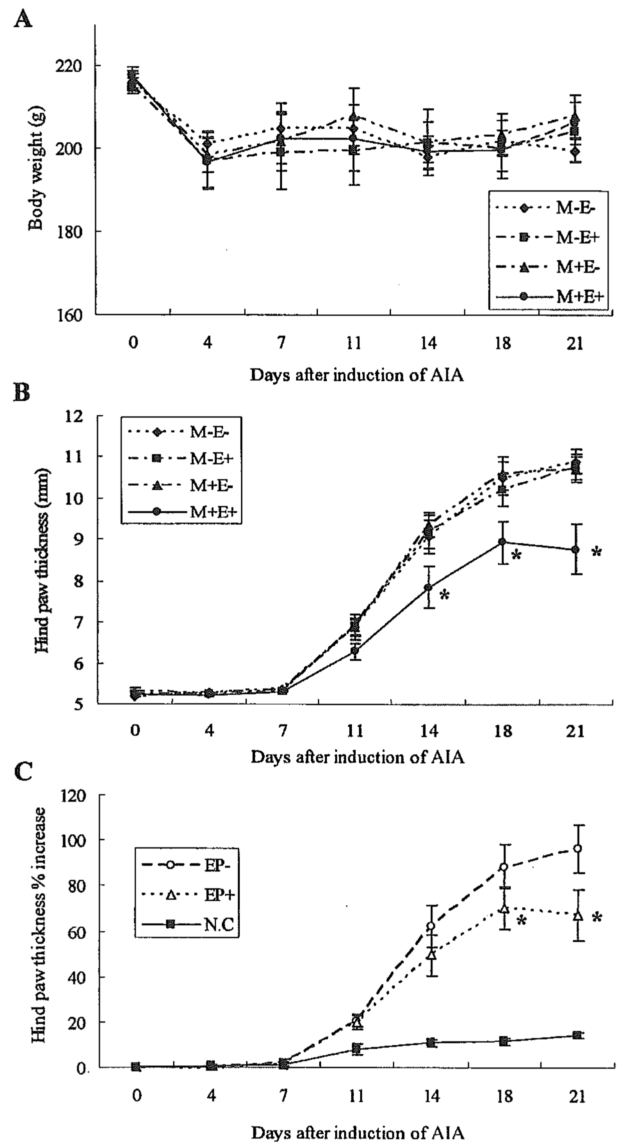

Figure 1. Effects of electrochemotherapy with methotrexate (MTX) on body weight and paw swelling in rats with adjuvant-induced arthritis (AIA). **A,** Weight loss was observed in all groups on day 4. There was no significant weight difference between the 4 groups throughout the entire study period. **B,** Left hind paw thickness, as measured by digital calipers, was maximal on day 21 in the M−/E− (no treatment; n = 9), M−/E+ (electroporation with saline; n = 10), and M+/E− (MTX without electroporation; n = 9) groups. The thickness of the left hind paw treated with electrical pulses after administration of MTX, 0.125 mg/kg/week (M+/E+; n = 8) was significantly decreased when compared with the other groups. * = $P < 0.05$ versus the M−/E−, M−/E+, and M+/E− groups. **C,** Effects of electrical pulses on paw swelling in the M+/E+ group. Electrical pulses were applied to the left hind paw only (electrically treated [EP+]) (n = 8), not the right paw (not electrically treated [EP−]) (n = 8). Application of electrical pulses after administration of low-dose MTX significantly inhibited hind paw swelling on days 18 and 21, as assessed by paw thickness and when compared with EP− paws. NC = negative control (non–adjuvant-injected model) (n = 5). * = $P < 0.05$ versus EP−. Bars show the mean ± SEM.

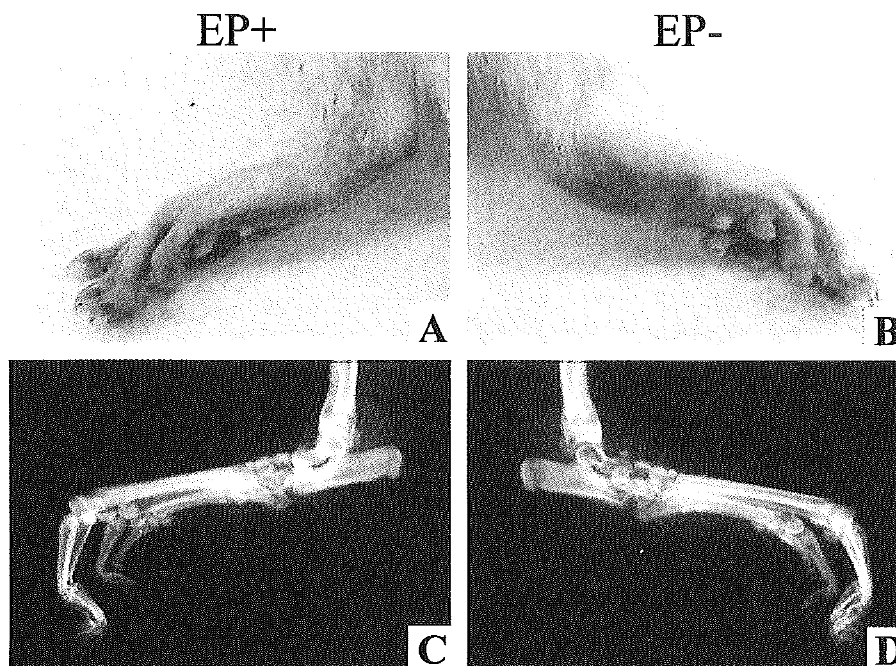

Figure 2. Gross appearance and radiographs of the hind paws of the same rat in the M+/E+ group on day 21. Following administration of MTX (0.125 mg/kg/week), electrical pulses were applied to the left hind paw only (EP+) (**A** and **C**). Note the obvious difference in the degree of swelling and joint damage between the left paw (EP+) and right paw (EP−) in gross appearance (**A** and **B**), as well as on soft x-ray (**C** and **D**). See Figure 1 for definitions.

changes in terms of radiodensity, subchondral bone erosion, periosteal reaction, and cartilage space were evaluated under blinded conditions by 2 rheumatologists (KI and TK) and graded on a 0–3 scale (where 0 = normal and 3 = severely damaged).

Histologic sections. Both hind paws were harvested from the animals for histopathologic examination. After the removal of skin, bones in the hind paws were decalcified in a neutral buffered 14% solution of EDTA/10% formalin, dehydrated in a graded ethanol series, embedded in paraffin, sectioned sagittally into 4-μm sections, and stained with hematoxylin and eosin or toluidine blue. Pathologic changes were evaluated by 2 observers according to a previously reported rating system (14), as follows: grade 0 = normal synovium, cartilage, and bone; grade 1 = hypertrophic synovium with cellular infiltration without pathologic change in bone and cartilage; grade 2 = pannus formation and cartilage erosion in addition to the hypertrophic synovium; grade 3 = additional severe erosion of cartilage and subchondral bone; grade 4 = loss of joint integrity and ankylosis.

In order to identify and count osteoclastic cells, sections were stained for tartrate-resistant acid phosphate (TRAP) using a staining kit (Sigma-Aldrich, St. Louis, MO). TRAP-positive multinucleated cells were counted in 11 selected fields (8 fields in the distal tibia and 3 fields in the talus), all at 100× magnification.

Statistical analysis. Body weight and hind paw thickness were evaluated by repeated analysis of variance and Fisher's protected least significant difference test. Pairwise comparisons were made using Wilcoxon's signed rank tests among groups. All statistical analyses were carried out using StatView software version 5.0 (SAS Institute, Cary, NC). *P* values less than or equal to 0.05 were considered significant.

RESULTS

Effects of electrochemotherapy on progression of AIA. No significant difference in body weight was noted between the 4 groups during the course of this experiment (Figure 1A), indicating that low-dose MTX, with or without electroporation, had little effect on the systemic physical condition of the rats with AIA.

The thickness of the hind paws in all rats was

Table 1. Radiologic and histologic scores and osteoclast numbers in rat AIA, 21 days after injection of adjuvant*

Group	Radiologic score (n = 8)	Histologic score (n = 8)	Osteoclast number (n = 5)
Right hind paw, EP-negative	3.8 ± 4.5	2.5 ± 1.2	77.6 ± 10.2
Left hind paw, EP-positive†	1.8 ± 2.2	1.3 ± 0.5	22.0 ± 2.4

* Values are the mean ± SD. AIA = adjuvant-induced arthritis; EP = electroporation.
† For all comparisons, $P < 0.05$ versus EP-negative.

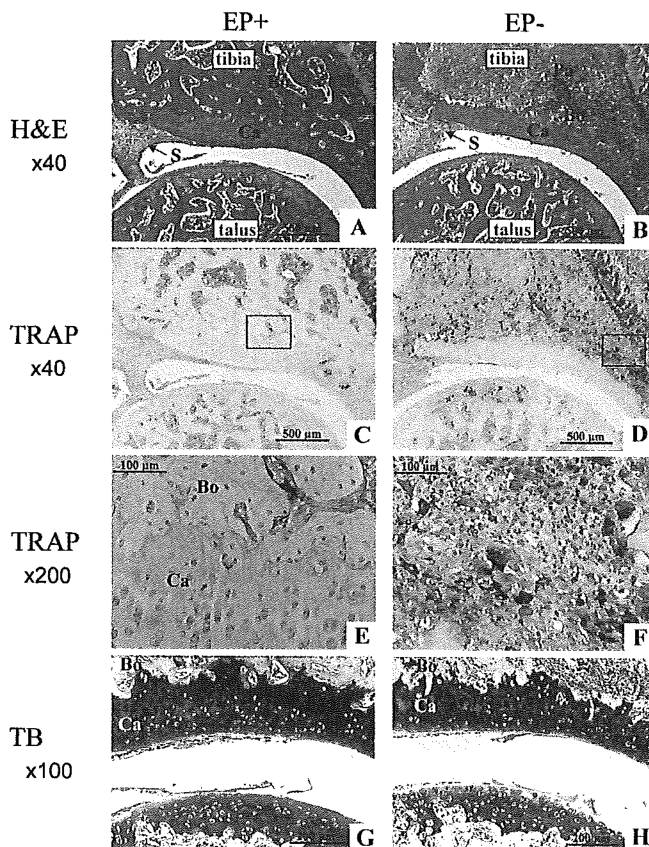

Figure 3. Histologic analysis of the ankle joints of the same rat in the M+/E+ group on day 21. **A** and **B,** Staining with hematoxylin and eosin (H&E). **C, D, E,** and **F,** Staining with tartrate-resistant acid phosphate (TRAP). **G** and **H,** Staining with toluidine blue (TB). The electroporation procedure was applied to the left ankle joint only (EP+) (**A, C, E,** and **G**). No inflammatory synovial tissue erosion into subchondral bone was observed with application of electroporation (**A**) compared with MTX only (**B**). Inflamed synovium infiltrated with lymphocytes was found to contain abundant osteoclastic multinucleated cells on TRAP staining (**D** and **F**). However, there was no difference in metachromasia of articular cartilage in the left and right hind paws. **E,** Higher-magnification view of the boxed area in **C. F,** Higher-magnification view of the boxed area in **D.** Bo = subchondral bone; Ca = cartilage; Pa = pannus; S = synovial tissue (see Figure 1 for other definitions).

significantly and consistently increased from day 11 until the end of the experiment. However, in the M+/E+ group, swelling of the left hind paw was significantly suppressed on days 14, 18, and 21 (Figure 1B) when compared with the 3 control groups (M+/E−, M−/E+, and M−/E−). The gross appearance of the hind paws is shown in Figures 2A and B. Thus, application of electrical pulses appeared to prevent the hind paw joints from progressing to advanced AIA. The degree of swelling differed significantly between the left (electrically treated [EP+]) and right (EP−) paws of the same rat in the M+/E+ group (Figure 1C).

Radiologic evaluation of bones and joints. Radiologic analysis revealed that the hind paw joints were severely damaged in the M−/E−, M−/E+, and M+/E− groups at 21 days after injection of the adjuvant. Therefore, at a dose of 0.125 mg/kg body weight, MTX did not prevent the joint damage (Figure 2D) or local swelling (Figure 2B) caused by progression of arthritis. In contrast, the radiologic damage score was significantly lower in the electrically treated left (EP+) hind paws in the M+/E+ group (Figures 2A and C and Table 1).

Histologic analyses. In the M+/E+ group, the histologic scores were significantly lower in the left hind paws (EP+) than in the right hind paws (EP−) (Figures 3A and B and Table 1). Inflamed synovial tissues with abundant lymphocytes were observed to erode into subchondral bone (Figure 3B). In sections of these joints, the population of TRAP-positive multinucleated osteoclastic cells was significantly lower in the bones of the left hind paw (EP+) than in those of the right hind paw (EP−) (Figures 3C, D, E, and F and Table 1). Toluidine blue staining revealed no degenerative changes of cartilage tissue, including irregularity of articular surface, disorganization of tidemark, and alternation of metachromasia, in either hind paw (Figures 3G and H).

DISCUSSION

These results indicate positive effects of pulsed electrical stimulation for attenuating arthritis by enhancing the antiarthritic effect of MTX. We believe that this is attributable to micropores created by the electrical pulses in the cytoplasmic membranes of cells in the synovium or other inflamed cells. The subsequent passive influx of MTX into the cells would attenuate the inflammatory responses that led to the AIA, although this study did not provide direct evidence of MTX influx. In this preliminary study, we could not identify the cells targeted by electrochemotherapy, and MTX-negative synovial cells, inflammatory cells, or both, may be targets for the drug.

The effects of electrical fields on living cells have been investigated since the 1960s, and high-voltage electrical pulses have been reported to generate transient and reversible pores in cell membranes. This phenomenon has been termed electroporation and is currently used to transfer genes or drugs into cells (6). Electrochemotherapy involves electroporation with drugs, and this methodology is used for the treatment of malignant tumors (5–9). The use of electrochemotherapy to introduce anticancer drugs into malignant tumors has been reported, e.g., bleomycin

for melanoma, basal cell carcinoma, Kaposi's sarcoma, squamous cell carcinoma (6), or chondrosarcoma (15). However, electrochemotherapy with MTX for the treatment of RA has not been reported, although the less-permeable character of MTX and its use as a DMARD in RA would make it an ideal candidate for this approach. Because the effect of pulsed electrical stimulation is expected only at the local site, this method might be applicable for an isolated joint with arthritis that is refractory to systemic chemotherapy or in the early stages of RA involving a limited number of joints without significant joint-destructive changes.

Clinical application of this therapy should not affect normal tissues. Using TUNEL staining, we did not observed any difference in the number of apoptotic cells between the M+/E+ and M+/E− groups (data not shown). We also confirmed in the pilot study that electrical pulses, used under the same conditions as those used in this experiment, did not influence the normal tissues of inbred 9-week-old male Lewis rats. In this pilot study, no inflammatory reactions were observed on histologic examination of the area treated with the electrical pulses, suggesting that electroporation under these conditions did not cause any damage to normal tissue, including cartilage, bone, muscle, and blood vessels (results not shown). However, the clinical application of electrochemotherapy requires further study, including the dose of MTX and the parameters of the electrical pulses.

This experimental study is limited in 2 key areas. First, electrochemotherapy was not applied to joints with established arthritis, and the effect of electrochemotherapy was estimated based on the progression of arthritis. This differs from the clinical situation, in which, as indicated previously (10,11), the inflammatory phase in this AIA model is self-limiting. Therefore, the efficacy of electrochemotherapy for the treatment of established chronic arthritis is difficult to determine in this model. Second, optimization of the application of pulsed electrical current may not be sufficient to obtain maximum delivery of MTX into cells and to achieve maximal antiinflammatory effect in RA. The conditions that enable the efficacy of electrical stimulation in electrochemotherapy may be quite different from the conditions used in the clinical treatment of malignancies that were reference sources for the present study. The potential value of electrochemotherapy for the treatment of RA has been illustrated by these studies, and further work is required to optimize electrochemotherapy to control disease in joints with RA refractory to treatment.

REFERENCES

1. Maini R, St Clair EW, Breedveld F, Furst D, Kalden J, Weisman M, et al, and the ATTRACT Study Group. Infliximab (chimeric anti-tumour necrosis factor α monoclonal antibody) versus placebo in rheumatoid arthritis patients receiving concomitant methotrexate: a randomised phase III trial. Lancet 1999;354:1932–9.
2. Lipsky PE, van der Heijde DM, St Clair EW, Furst DE, Breedveld FC, Kalden JR, et al, and the Anti-Tumor Necrosis Factor Trial in Rheumatoid Arthritis with Concomitant Therapy Study Group. Infliximab and methotrexate in the treatment of rheumatoid arthritis. N Engl J Med 2000;343:1594–602.
3. Furst DE, Kremer JM. Methotrexate in rheumatoid arthritis. Arthritis Rheum 1988;31:305–14.
4. Multicenter evaluation of synovectomy in the treatment of rheumatoid arthritis: report of results at the end of three years. Arthritis Rheum 1977;20:765–71.
5. Heller R, Gilbert R, Jaroszeski MJ. Clinical applications of electrochemotherapy. Adv Drug Deliv Rev 1999;35:119–29.
6. Mir LM, Orlowski S. Mechanisms of electrochemotherapy. Adv Drug Deliv Rev 1999;35:107–18.
7. Hyacinthe M, Jaroszeski MJ, Dang VV, Coppola D, Karl RC, Gilbert RA, et al. Electrically enhanced drug delivery for the treatment of soft tissue sarcoma. Cancer 1999;85:409–17.
8. Horiuchi A, Nikaido T, Mitsushita J, Toki T, Konishi I, Fujii S. Enhancement of antitumor effect of bleomycin by low-voltage in vivo electroporation: a study of human uterine leiomyosarcomas in nude mice. Int J Cancer 2000;88:640–4.
9. Gothelf A, Mir LM, Gehl J. Electrochemotherapy: results of cancer treatment using enhanced delivery of bleomycin by electroporation. Cancer Treat Rev 2003;29:371–87.
10. Welles WL, Silkworth J, Oronsky AL, Kerwar SS, Galivan J. Studies on the effect of low dose methotrexate on rat adjuvant arthritis. J Rheumatol 1985;12:904–6.
11. Kawai S, Nagai K, Nishida S, Sakyo K, Murai E, Mizushima Y. Low-dose pulse methotrexate inhibits articular destruction of adjuvant arthritis in rats. J Pharm Pharmacol 1997;49:213–5.
12. Morgan SL, Baggott JE, Bernreuter WK, Gay RE, Arani R, Alarcon GS. MTX affects inflammation and tissue destruction differently in the rat AA model. J Rheumatol 2001;28:1476–81.
13. Clark RL, Cuttino JT Jr, Anderle SK, Cromartie WJ, Schwab JH. Radiologic analysis of arthritis in rats after systemic injection of streptococcal cell walls. Arthritis Rheum 1979;22:25–35.
14. Shiozawa S, Shimizu K, Tanaka K, Hino K. Studies on the contribution of c-fos/AP-1 to arthritic joint destruction. J Clin Invest 1997;99:1210–6.
15. Shimizu T, Nikaido T, Gomyo H, Yoshimura Y, Horiuchi A, Isobe K, et al. Electrochemotherapy for digital chondrosarcoma. J Orthop Sci 2003;8:248–51.

ARTHRITIS & RHEUMATISM
Vol. 52, No. 1, January 2005, pp 155–163
DOI 10.1002/art.20713
© 2005, American College of Rheumatology

Use of Bone Morphogenetic Protein 2 and Diffusion Chambers to Engineer Cartilage Tissue for the Repair of Defects in Articular Cartilage

Masashi Nawata,[1] Shigeyuki Wakitani,[1] Hiroyuki Nakaya,[2] Akira Tanigami,[3] Toyokazu Seki,[3] Yukio Nakamura,[1] Naoto Saito,[1] Kenji Sano,[1] Eiko Hidaka,[1] and Kunio Takaoka[4]

Objective. **To examine the ability of cartilage-like tissue, generated ectopically in a diffusion chamber using recombinant human bone morphogenetic protein 2 (rHuBMP-2), to repair cartilage defects in rats.**

Methods. **Muscle-derived mesenchymal cells were prepared by dissecting thigh muscles of 19-day postcoital rat embryos. Cells were propagated in vitro in monolayer culture for 10 days and packed within diffusion chambers (10^6/chamber) together with type I collagen (CI) and 0, 1, or 10 μg rHuBMP-2, and implanted into abdominal subfascial pockets of adult rats. Tissue pellets were harvested from the diffusion chambers at 2 days to 6 weeks after implantation, and examined by histology, by reverse transcription–polymerase chain reaction (PCR) for aggrecan, CII, CIX, CX, and CXI, MyoD1, and core binding factor a1/runt-related gene 2, and by real-time PCR for CII. Tissue pellets generated in the chamber 5 weeks after implantation were transplanted into a full-thickness cartilage defect made in the patellar groove of the same strain of adult rat.**

Results. **In the presence of 10 μg rHuBMP-2, muscle-derived mesenchymal cells expressed CII messenger RNA at 4 days after transplantation, and a mature cartilage mass was formed 5 weeks after transplantation in the diffusion chamber. Cartilage was not formed in the presence of 1 μg rHuBMP-2 or in the absence of rHuBMP-2. Defects receiving cartilage engineered with 10 μg rHuBMP-2 were repaired and restored to normal morphologic condition within 6 months after transplantation.**

Conclusion. **This method of tissue engineering for repair of articular defects may preclude the need to harvest cartilage tissue prior to mosaic arthroplasty or autologous chondrocyte implantation. Further studies in large animals will be necessary to validate this technique for application in clinical practice.**

Regeneration of articular cartilage is a challenging subject for research on joint surgery (1), and several methods have been devised and attempted in clinical practice to repair focal defects in articular cartilage, especially in young patients (2–5). Currently, mosaic arthroplasty (6), a procedure in which pieces of autogeneic chondro-osseous mass are procured from peripheral parts of the joint surface and transplanted into the focal cartilage defects, is often used with success in the knee joint (7). However, a number of limitations persist, and these include the limited source of the autogeneic osteochondral tissue mass and the potential risk of progression to osteoarthritis due to the injury caused by procurement of graft tissue from the normal joint surface. In addition, the functional durability of the repaired cartilage and the limited application of the approach to small joints are further areas of concern.

Recently, technologies have been developed in order to fabricate tissues for the repair of skeletal defects. The transplantation of chondrocytes of auto- or allogeneic origin has been demonstrated in both experimental (8–11) and clinical (12) situations. In these

Supported in part by a Grant-in-Aid for Scientific Research from the Japanese Ministry of Education, Culture, Sports, Science and Technology (16390436).

[1]Masashi Nawata, MD, Shigeyuki Wakitani, MD, PhD, Yukio Nakamura, MD, Naoto Saito, MD, PhD, Kenji Sano, PhD, Eiko Hidaka, PhD: Shinshu University School of Medicine, Matsumoto, Japan; [2]Hiroyuki Nakaya, MD: Osaka University Medical School, Osaka, Japan; [3]Akira Tanigami, MD, PhD, Toyokazu Seki, PhD: Otsuka Pharmaceutical Company, Tokushima, Japan; [4]Kunio Takaoka, MD, PhD: Osaka City University Medical School, Osaka, Japan.

Address correspondence and reprint requests to Shigeyuki Wakitani, MD, PhD, Department of Orthopaedic Surgery, Shinshu University School of Medicine, 3-1-1 Asahi, Matsumoto 390-8621, Japan. E-mail: wakitani@hsp.md.shinshu-u.ac.jp.

Submitted for publication May 6, 2004; accepted in revised form September 14, 2004.

cases, cells are dissociated from pieces of articular cartilage, propagated (or left unpropagated) on dishes in ex vivo conditions to expand the cell population, and then transplanted with or without scaffolding carrier materials into the cartilage defect of the recipient. Although these methods can repair cartilage defects, some difficulties persist. Allogeneic transplantation has the inherent risks of disease transmission and rejection; autologous transplantation causes damage to the donor site.

In an effort to address the limitations of existing approaches, we attempted to generate cartilage tissue by inducing the differentiation of muscle-derived cells into the chondrocytic lineage in an in vivo environment with recombinant human bone morphogenetic protein 2 (rHuBMP-2). Articular defects in rat joints that received the induced cartilage-like tissue were repaired and restored to normal condition. The present report provides evidence to support this approach for the successful treatment of articular cartilage defects.

MATERIALS AND METHODS

Preparation of muscle-derived mesenchymal cells and diffusion chambers. Mesenchymal cells were obtained from the thigh muscles of 19-day, postcoital, F344 rat embryos (purchased from Japan SLC, Hamamatsu, Japan). The muscle tissues were minced with scissors and digested in 0.25% trypsin with 1 m*M* EDTA-Na_4 (Invitrogen, Carlsbad, CA). The dissociated cells were propagated on plastic culture dishes (10 cm in diameter) in Dulbecco's modified Eagle's medium (Invitrogen) supplemented with 10% (volume/volume) fetal calf serum (Invitrogen) and antibiotics (mixture of 5 mg/ml penicillin G, 5 mg/ml streptomycin, 10 mg/ml neomycin; Invitrogen) and passaged under routine culture conditions for 10 days. At the end of this period, the cells were detached from the dishes with 0.25% trypsin with 1 m*M* EDTA-Na_4 and packed within diffusion chambers (10^6 cells/chamber).

In order to construct a diffusion chamber for cell transplantation, a diffusion chamber kit (Millipore, Billerica, MA), consisting of a plastic ring (14 mm in outer diameter and 10 mm in inner diameter), a membrane filter (comprising a mixture of cellulose acetate and cellulose nitrate [0.45 μm in pore size]), and adhesive sealant, was utilized. The inner diameter of the ring was reduced to 5 mm by inserting another plastic ring. Only one side of the larger plastic ring was initially sealed with a membrane filter and adhesive sealant. For the next step, 40 μl of 0.3% (weight/weight) pig type I collagen (Cellmatrix LA; Nitta Gelatin, Osaka, Japan) and 0, 1, or 10 μg of rHuBMP-2 (Yamanouchi Pharmaceutical, Tokyo, Japan) were introduced into the diffusion chamber. The chamber was then freeze-dried and sterilized with ethylene oxide gas.

After these processes were completed, 10^6 cells suspended in 40 μl of serum-free culture medium containing 0.3% (w/w) pig type I collagen (Cellmatrix I-A; Nitta Gelatin) were introduced into the diffusion chamber, and another open side of the chamber was sealed with a filter and adhesive sealant. Sixty-two chambers (42 for histologic examination, 8 for reverse transcription–polymerase chain reaction [RT-PCR] analysis, and 12 for real-time PCR analysis) with 10 μg of rHuBMP-2 (group B10), 10 chambers (all for histologic examination) with 1 μg of rHuBMP-2 (group B1), and 46 chambers (26 for histologic examination, 8 for RT-PCR analysis, and 12 for real-time PCR analysis) without rHuBMP-2 (group B0) were prepared for analysis and implantation.

Transplantation of the diffusion chamber into the abdominal pocket of rats. Immediately after loading the cells into the diffusion chambers, each chamber was surgically inserted into a pocket in the abdominal muscles of 8-week-old F344 rats under diethyl ether anesthesia. After surgery, the rats were housed in cages and were given free access to standard chalk-like food and water. At 2, 4, 6, 8, 14, 21, 28, 35, and 42 days after implantation, the animals were killed in due order and the diffusion chambers were harvested (Table 1) for histologic examination. For RT-PCR analysis, 2 chambers were harvested at 2-, 4-, 7-, and 14-day intervals after implantation. For real-time PCR analysis, 2 chambers were harvested at 2-, 4-, 6-, 14-, 28-, and 42-day intervals after implantation.

Harvested tissue pellets within the chambers were inspected for vascular invasion caused by seal failure or breakage of the filter membranes. When vascular invasion was noted, the tissue was excluded from the transplantation into the cartilage defect and from PCR analysis. The tissue pellets for histologic examination were radiographed and fixed in 20% neutral buffered formalin solution, prior to processing for histologic examination. Some parts of the tissue pellet from the 5-week-old sample were used for transplantation into the rat-knee defect. Tissue pellets for RT-PCR or real-time PCR were frozen in liquid nitrogen immediately after harvesting.

Transplantation of tissue pellets from diffusion chambers into osteochondral defects of rats. Some portions of the tissue pellet removed from the diffusion chambers at 5 weeks after implantation were transplanted into cartilage defects generated on the patellar grooves of the knee joints of 7 (4 from group B10, 3 from group B0) mature, same-strain rats (a quarter tissue pellet/animal). The transplantation procedure was performed with the rats under anesthesia, using an intramuscular injection of a mixture of ketamin (100 mg/ml, 0.6

Table 1. Cartilage formation in diffusion chamber*

	rHuBMP-2			Area of cartilage tissue in cross-section
	0 μg	1 μg	10 μg	
2 days	0/2	–	0/2	–
4 days	0/2	–	0/2	–
6 days	0/2	–	0/2	–
8 days	0/2	–	0/2	–
14 days	0/2	–	0/2	–
21 days	0/4	–	4/6	1/4
28 days	0/4	0/4	9/10	1/3
35 days	0/4	0/6	9/10	Almost all
42 days	0/4	–	6/6	Almost all

* Except where indicated otherwise, values are the number of samples with cartilage formation/number of experiments. rHuBMP-2 = recombinant human bone morphogenetic protein 2.